Atomistic Modeling of Solid State Hydrogen Storage Materials

SAND2019-12151C

236st Electrochemical Society (ECS), October 13-17, 2019, Atlanta, George

Crosscutting Materials Innovation for Transformational Chemical and Electrochemical Energy Conversion Technologies (I05)

Section 3: State-of-the-art in Energy Materials Theory and Computation

X. W. Zhou[1], D. C. Spataru[1], S. Kang[2], T. W. Heo[2], B. C. Wood[2], V. Stavila[1], and M. D. Allendorf[1]

[1]Sandia National Laboratories, [2]Lawrence Livermore National Laboratory, Livermore, California 94550, USA

Sandia National Laboratories is a multimission laboratory managed and operated by National Technology & Engineering Solutions of Sandia, LLC, a wholly owned subsidiary of Honeywell International Inc., for the U.S. Department of Energy's National Nuclear Security Administration under contract DE-NA0003525. A portion of this work was performed under the auspices of Lawrence Livermore National Laboratory under Contract DE-AC52-07NA27344. The authors gratefully acknowledge research support through the Hydrogen Storage Materials—Advanced Research Consortium (HyMARC), from the U.S. Department of Energy, Office of Energy Efficiency and Renewable Energy, Fuel Cell Technologies Office, under Contract Numbers DE-AC04-94AL85000 and DE-AC52-07NA27344. Discussions with J. A. Zimmerman, N. Bartelt, R. Sills, D. Robinson, and D. Cowgill are also highly appreciated. The views, opinions, findings, and conclusions stated herein are those of the authors and do not necessarily reflect those of CRDF Global, or the United States Government or any agency thereof. Neither the United States Government nor any agency thereof, nor any of their employees, makes any warranty, expressed or implied, or assumes any legal liability or responsibility for the accuracy, completeness, or usefulness of any information, apparatus, product, or process disclosed, or represents that its use would not infringe privately owned rights.

Research Background

- **Hydrogen is an excellent, efficient, and clean energy carrier**
- **Metal hydrides draw interests due to an ideal combination of volumetric and gravimetric densities**

Main commercial challenges:

- ❑ Overall kinetics is sluggish
- ❑ Rate-limiting mechanisms are not clear
- ❑ Phase transformation mechanisms are not understood

Source: https://ssl.toyota.com/mirai/stations.html

Hydrogen Materials Advanced Research Consortium

www.hymarc.org

Theory, simulation, & data

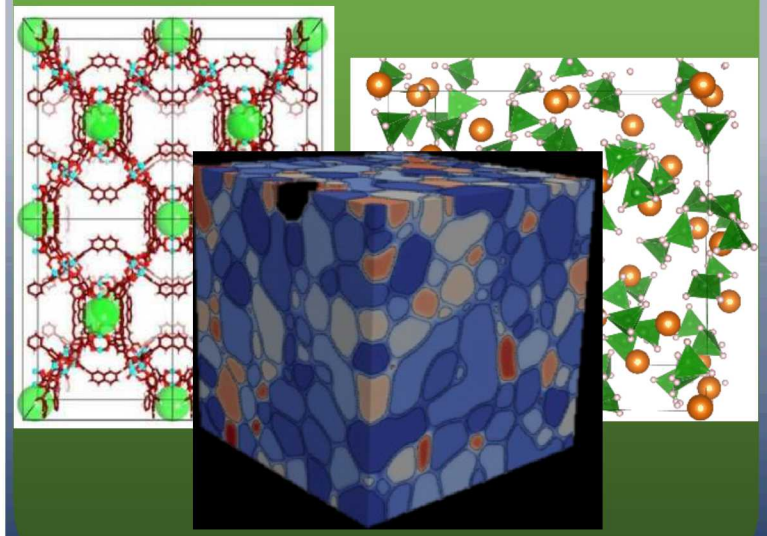

Controlled synthesis

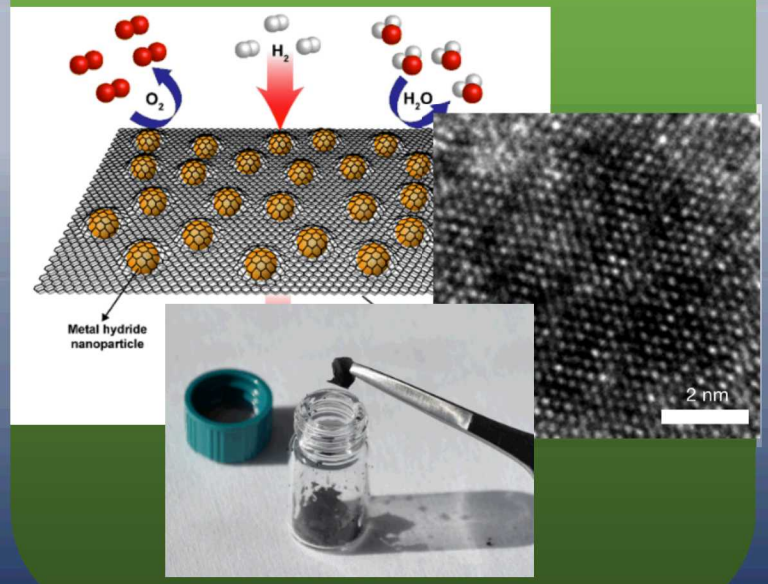

In situ characterization

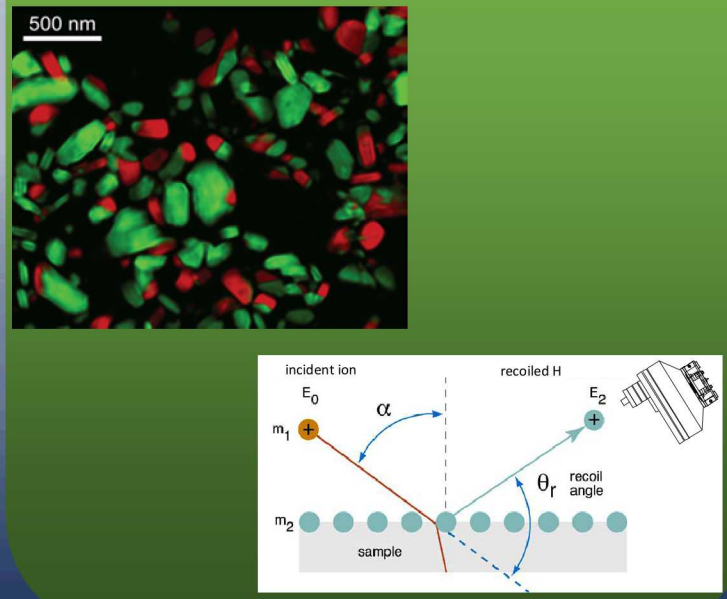

HyMARC provides **tools** and **foundational understanding** of thermodynamics and kinetics needed to improve solid-state hydrogen storage materials

Role of Atomistic Simulations

Continuum models require knowledges on

- **Evolution of bulk properties such as Gibbs energy, lattice / elastic constants, and diffusivities**
- **Evolution of surface / interface properties such as surface / interface energies, surface segregation, diffusivities**
- **Reaction mechanisms**

These can be obtained from atomistic simulations but not other ways

Outline: Three Classes of Materials

- **Diffusional hydride PdH_x**
  - Bulk properties (Gibbs energy, lattice / elastic constants, diffusivities)
  - Surface / interface properties (surface / interface energies, surface segregation, diffusivities)
- **Transformational hydride MgH_x**
  - Bond order potential development
  - Molecular dynamics simulation examples
- **Complex hydride MgB_xH_y**
  - Interatomic potential development
  - Molecular dynamics simulation examples

Molecular Dynamics (MD) Uncertainty Quantification

The total MD simulated time t_{tot} is divided into N segments $t_i = i\Delta t$ ($i = 1, 2, \ldots, N$, $\Delta t = t_{tot}/N$). Each segment gives a time averaged property P_i. The best estimate of the property is $\bar{P} = \sum_{i=1}^{N} P_i/N$. The uncertainty of $\bar{P}$ can be quantified by the standard deviation defined as

$$\sigma = \sqrt{\frac{\sum_{i=1}^{N}(P_i - \bar{P})^2}{(N-1)N}}$$

Alternatively, if $\bar{P}_i$ are obtained from different properties $i = 1, 2, \ldots, n$, then the uncertainty can also be quantified by

$$\sigma = \sqrt{\frac{\sum_{i=1}^{n}(\bar{P}_i - P^*)^2}{n}}$$

where P^* is a knowledge based best estimate. For example, if $\bar{P}_i$ are elastic constants $\overline{C_{11}}$, $\overline{C_{22}}$, $\overline{C_{33}}$ calculated for cubic crystals, $P^* = (\overline{C_{11}}+\overline{C_{22}} + \overline{C_{33}})/n$, $n = 3$. If $\overline{D_i}$ are diffusivities calculated at different temperatures T_i ($i = 1, 2, \ldots, n$), then we can define $\bar{P}_i$ as $\ln(\overline{D_i})$ and P^* as $\ln(D_0) - Q/kT_i$, with D_0 the pre-exponential factor and Q the activation energy.

First Class: Diffusional Hydrides

Case Study: PdH_x

PdH_x: Selection of Pd-H Potential

Reference	Miscibility Gap	Selection
Y. H. Park et al, J. Mol. Model, 23, 108 (2017).	Yes	Not tried
D. Fukushi et al, Jp. J. Appl. Phys. I, 39, 1953 (2000).	Pair potential	Not selected
R. J. Wolf et al, Phys. Rev. B, 48, 12415 (1993).	Yes	Not available
R. J. Wolf et al, Phys. Rev. B, 46, 8027 (1992).	Yes	Not available
X. W. Zhou et al, J. Mater. Res., 23, 704 (2008).	Yes	Selected

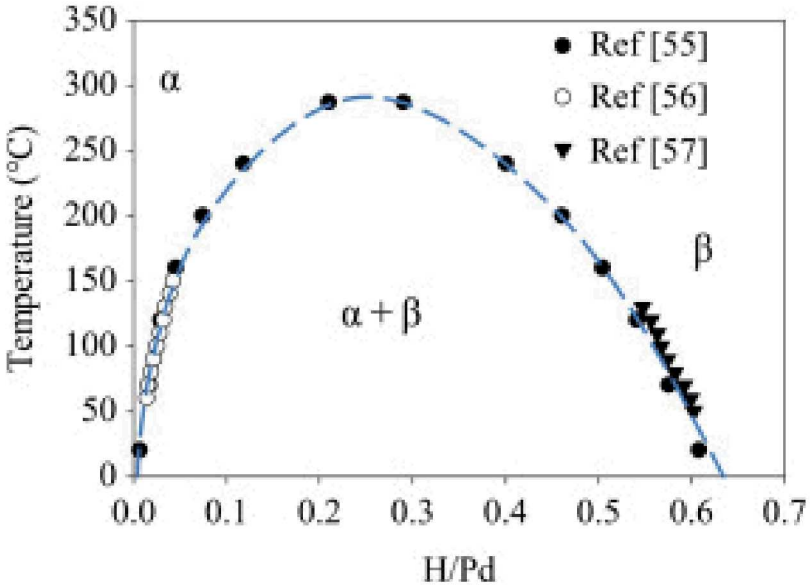

- The key is to capture the miscibility gap
- This is a challenge for interatomic potentials
- Wolf et al's potential captured it, but is lost
- Our potential also captures it and is used

N. A. Al-Mufachi et al, Ren. Sus. Ener. Rev., 47, 540 (2015)

PdH_x: Diffusion Analysis Method

- Coordinates of N hydrogen atoms (i = 1, 2, …, N) at t = jΔt, j = 1, 2, …, m (m = $t_{MD}/\Delta t$) are $\alpha_i(t)$.
- m+1-k displacement measurements for hydrogen atom i over a kΔt period: $\Delta\alpha_{i,j}(k\Delta t) = \alpha_i(j\Delta t - \Delta t + k\Delta t) - \alpha_i(j\Delta t - \Delta t)$ where j = 1, 2, …, m+1-k.
- This allows calculations of hydrogen mean square displacement
- Mean square displacement is fitted to diffusivities D

$$\left\langle \left[\Delta\alpha(k\Delta t)\right]^2 \right\rangle = \frac{\sum_{i=1}^{N}\sum_{j=1}^{m+1-k}\left[\Delta\alpha_{i,j}(k\Delta t)\right]^2}{N(m+1-k)}$$

$$\left\langle \left[\Delta\alpha(k\Delta t)\right]^2 \right\rangle = 2D_\alpha t$$

$$\left\langle \left[\Delta x(k\Delta t)\right]^2 \right\rangle + \left\langle \left[\Delta z(k\Delta t)\right]^2 \right\rangle = 4D_{xz} t$$

$$\left\langle \left[\Delta x(k\Delta t)\right]^2 \right\rangle + \left\langle \left[\Delta y(k\Delta t)\right]^2 \right\rangle + \left\langle \left[\Delta z(k\Delta t)\right]^2 \right\rangle = 6D_{xyz} t$$

MSD

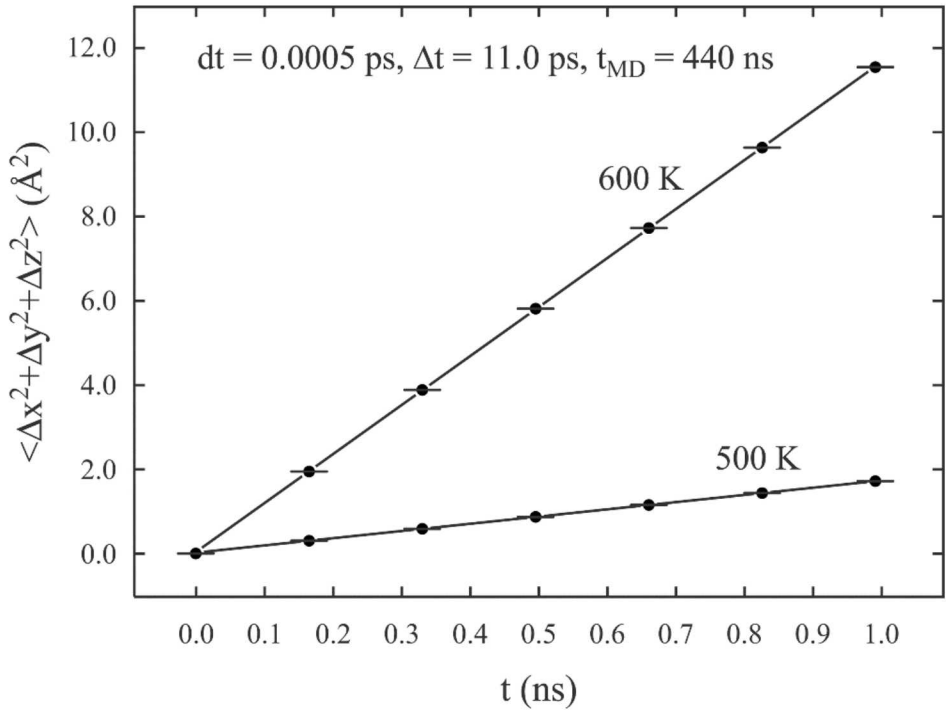

PdH_x: Bulk Diffusion

t_{MD} = 2.2 ns

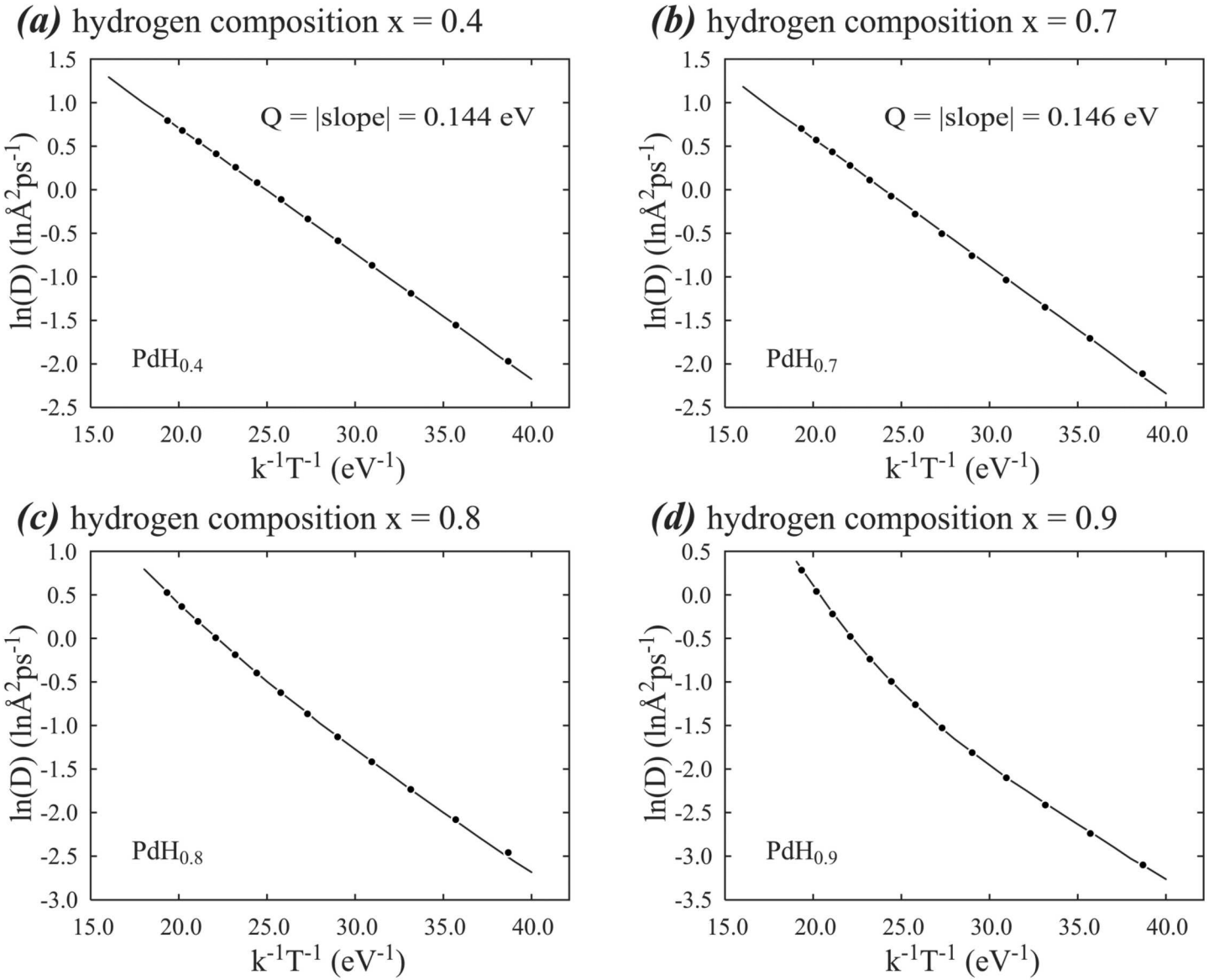

- Statistical errors are negligible
- MD results fall exactly on smooth lines
- The MD does not have time and length scale issues
- The Arrhenius relation is satisfied at low H concentrations
- The ln(D) vs. 1/T relation becomes non-linear at high H concentrations

PdH_x: Experimental Validation

Table I. Measured and predicted activation energy Q and pre-exponential factor D_0 as a function of phase and temperature.

Authors	Phase	T (K)	Q (eV)	D_0 (Å^2/ps)
Arons et al [2,3]	β	110-300	0.210	---
		50-100	0.150	---
Cornell et al [4]	β	195-300	0.228	---
		100-195	0.100	---
Mazzolai et al [5]	β	250-270	0.210	---
		130-200	0.130	---
Burger et al [6]	β	230-320	0.210	---
		180-230	0.060	---
Torrey et al [7]	β	>220	0.240	---
		<220	0.080	---
Beg et al [15]	β	293-473	0.146	1.10×10^{1}
Seymour et al [16]	β	296-413	0.229	9.30×10^{0}
Davis et al [17]	β	300-400	0.228	3.00×10^{1}
Majorowski et al [18]	β	208-338	0.287	1.13×10^{2}
Bucur [19]	α	278-323	0.054	2.48×10^{1}
Holleck [20]	α	533-913	0.055	2.94×10^{1}
Simmons et al [21]	α	273-650	0.062	6.10×10^{1}
Maeda et al [22]	α	773-1373	0.215	2.80×10^{1}
Hara et al [23]	α	523-773	0.219	2.40×10^{1}
Pietrzak et al [24,25]	α	273-473	0.230	2.20×10^{1}
Yoshihara et al [26]	α	273-350	0.231	2.91×10^{1}
Zuchner [27]	α	200-700	0.250	5.25×10^{1}
MD fitted Eqs. (1) - (5)	α	300-600	~0.15	$\sim3.5\times10^{1}$
	β (x=0.8)	600	~0.20	$\sim7.8\times10^{1}$
	β (x=0.8)	300	~0.14	$\sim1.7\times10^{1}$

X. W. Zhou, T. W. Heo, B. C. Wood, V. Stavila, S. Kang, and M. D. Allendorf, Scr. Mater., 149, 103 (2018)

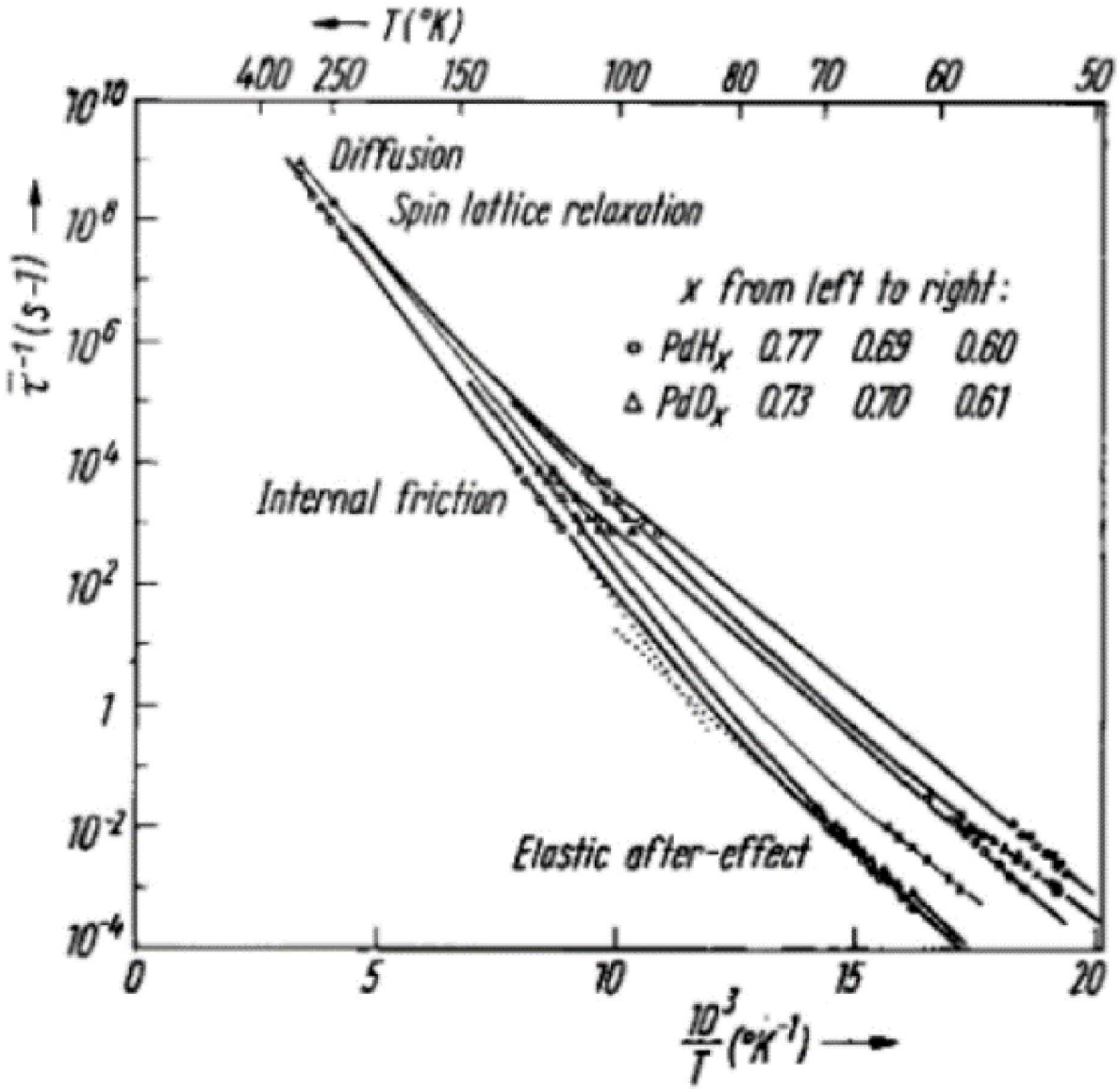

Arons et al, Phys. Stat. Sol. 1970, 40, 107

PdH_x: Two Representative Jump Paths

Barrier calculated by nudged elastic band

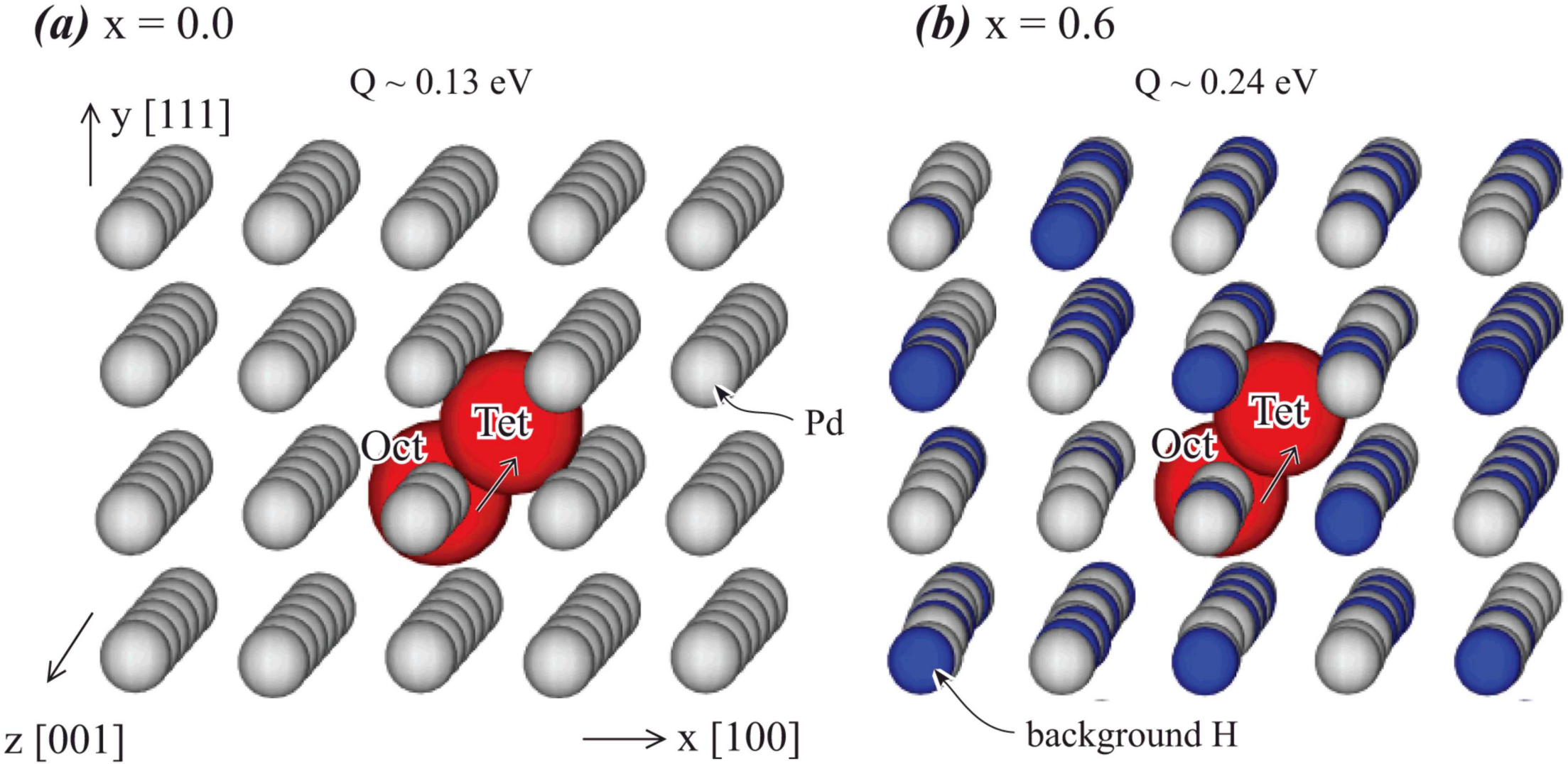

PdH_x: Two-Barrier Model

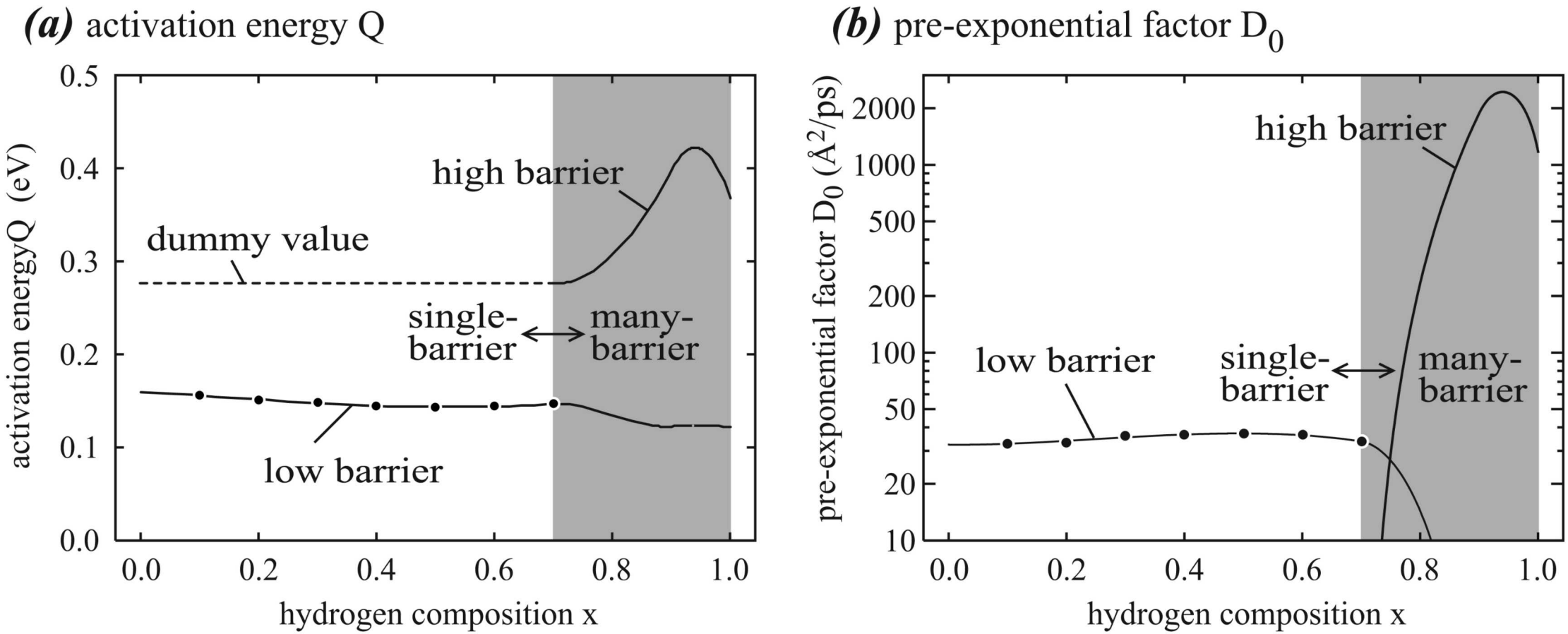

$$D = D_{0,1} \cdot \exp\left(-\frac{Q_{0,1}}{kT}\right) + D_{0,2} \cdot \exp\left(-\frac{Q_{0,2}}{kT}\right)$$

PdH_x: Two-Barrier Model at Surface

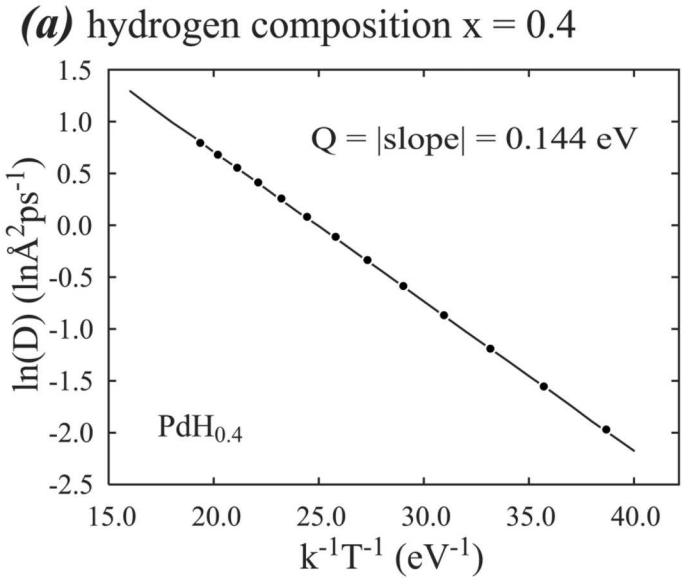

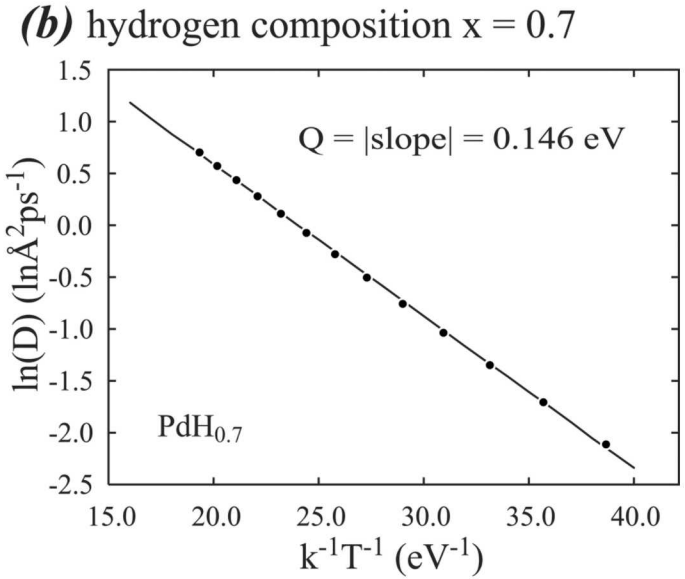

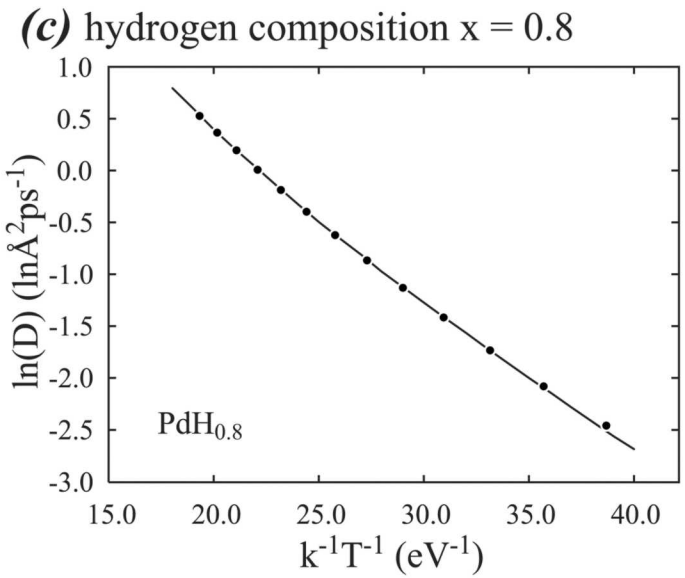

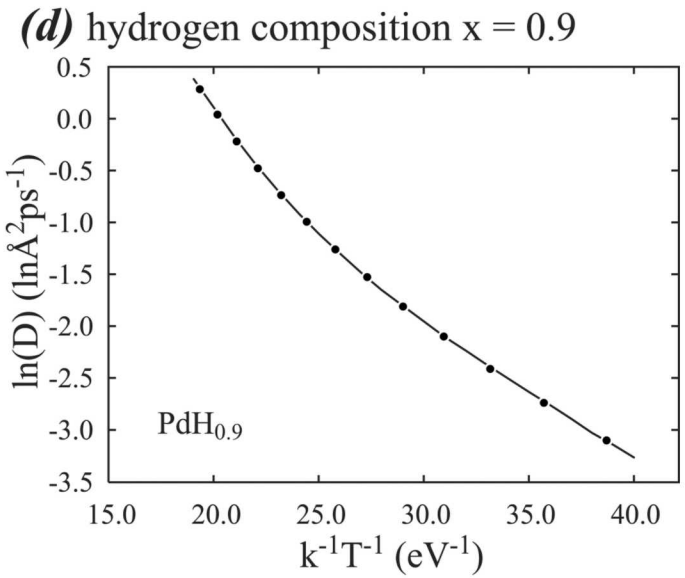

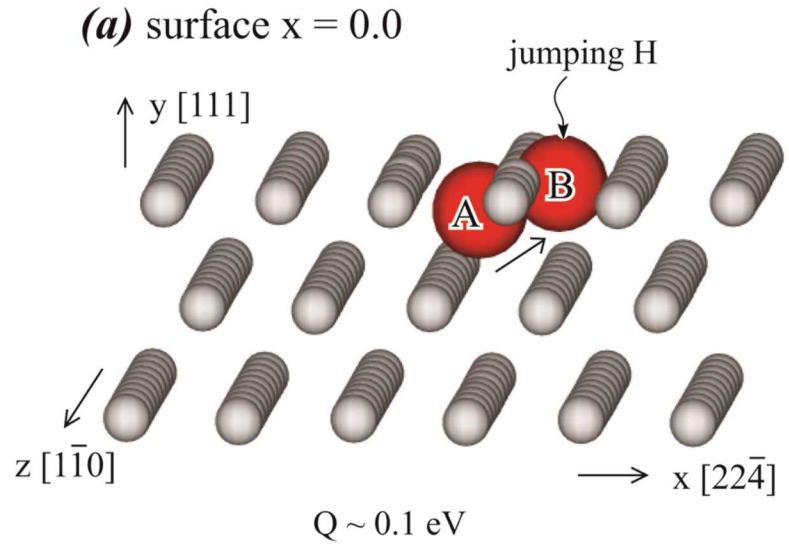

Q ~ 0.1 eV

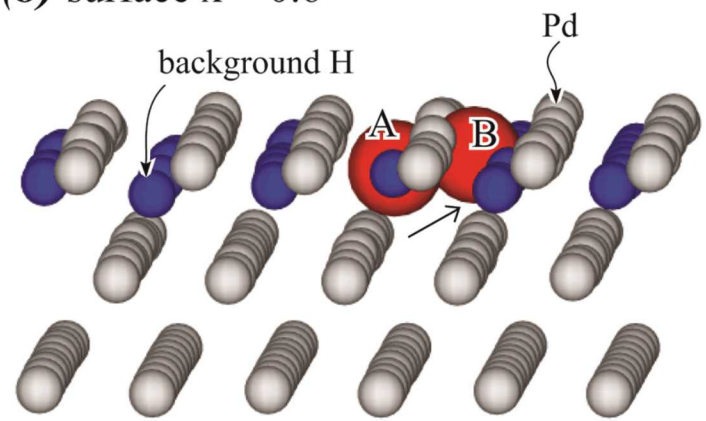

Q ~ 0.3 eV

PdH_x: Finite-Temperature Elastic Constants

Convergence is extremely challenging

MD calculations:

$$C_{ij,MD} = \frac{\left\langle \sigma_i\left(+\varepsilon_j\right)\right\rangle - \left\langle \sigma_i\left(-\varepsilon_j\right)\right\rangle}{2\varepsilon_j}, \qquad i = 1,2,\ldots,6$$

Cast to cubic values

$$C_{ii} = \frac{C_{11,MD} + C_{22,MD} + C_{33,MD}}{3}, \qquad i = 1-3$$

$$C_{ii} = \frac{C_{44,MD} + C_{55,MD} + C_{66,MD}}{3}, \qquad i = 4-6$$

$$C_{ij} = C_{ji} = \frac{C_{12,MD} + C_{13,MD} + C_{21,MD} + C_{23,MD} + C_{31,MD} + C_{32,MD}}{6}, \qquad j > i, j = 2-3$$

$$C_{ij} = C_{ji} = 0, \qquad j > i, j = 4-6$$

t_{MD} = 100 ns (first 20 ns discarded)

PdH_x: Elastic Constants

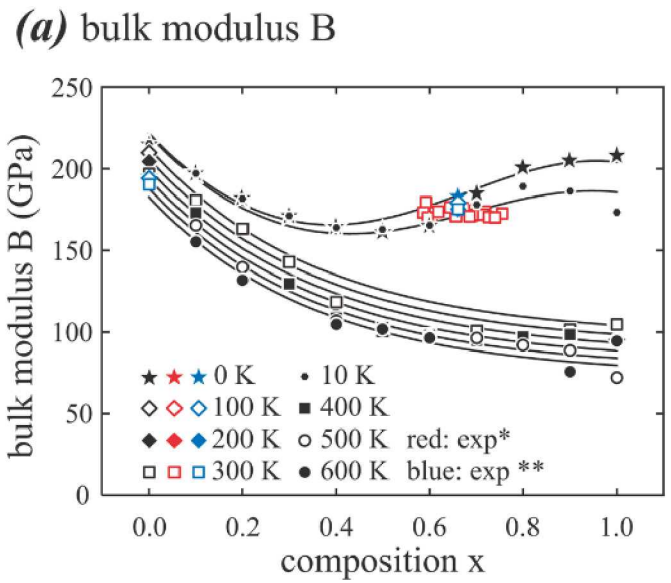

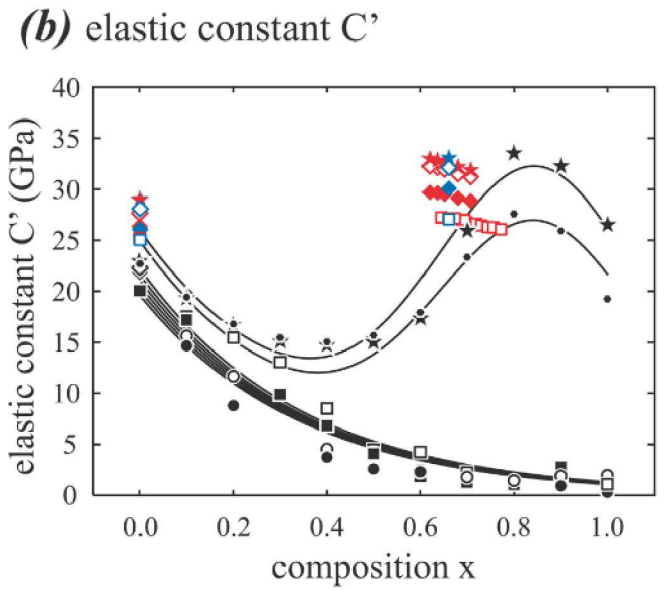

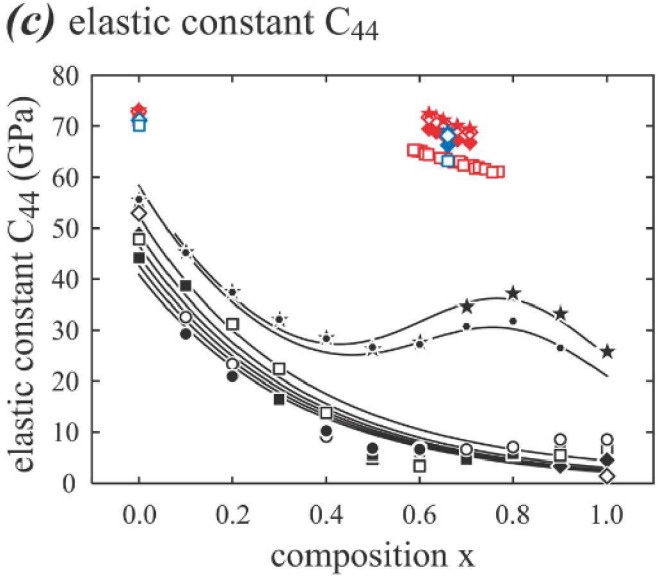

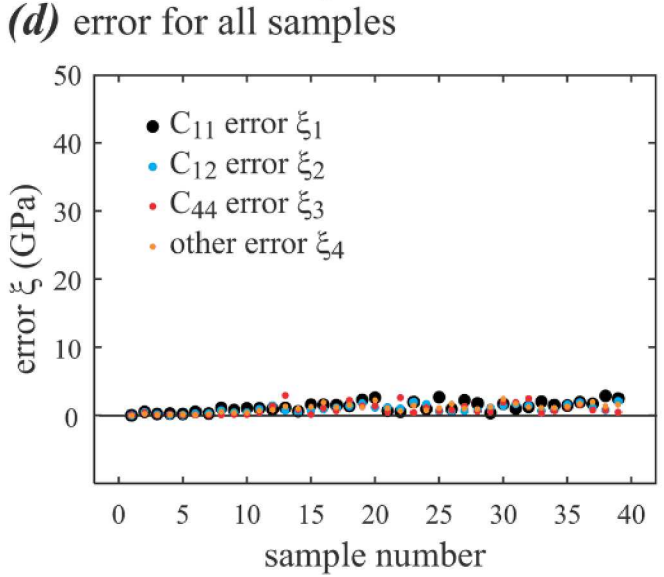

- **Trends cannot be attributed to potentials**
- **Experimental values pertain to ultrasonic measurements**
- **MD pertains to mechanical testing with continuous Pd-H debonding**
- **Significant difference between static and dynamic elastic constants is well known for minerals (Int. J. Rock Mech. Sci. Geomech. Abstr. 1988, 25, 479; METABK 2003, 42, 37-39)**

* R. B. Schwarz et al, Acta Mater. 54, 569 (2005)
* D. G. Safarik et al, Ultrasonics. 50, 155 (2010)
** Hsu, D. K.; Leisure, R. G. Phys. Rev. B. 20, 1339 (1979)

PdH_x: Simulation of Dynamic C_{44}

Sinoidal loading in MD (ι: thermal noise): $\sigma_i + \iota = C_{ij} \cdot \left[\varepsilon_{j,0} + \Delta\varepsilon_j \sin\left(2\pi \frac{t}{\tau} \right) \right]$

Linear $\langle(\sigma_i+\iota)^2\rangle$ vs. $\Delta\varepsilon^2_j$ relation: $\left\langle (\sigma_i + \iota)^2 \right\rangle = C_{ij}^2 \cdot \left\langle \left[\varepsilon_{j,0} + \Delta\varepsilon_j \sin\left(2\pi \frac{t}{\tau} \right) \right]^2 \right\rangle = \frac{C_{ij}^2}{2} \Delta\varepsilon_j^2 + C_{ij}^2 \cdot \varepsilon_{j,0}^2$

(a) Pd $\langle(\sigma_4+\iota)^2\rangle$ vs. $\Delta\varepsilon^2_4$

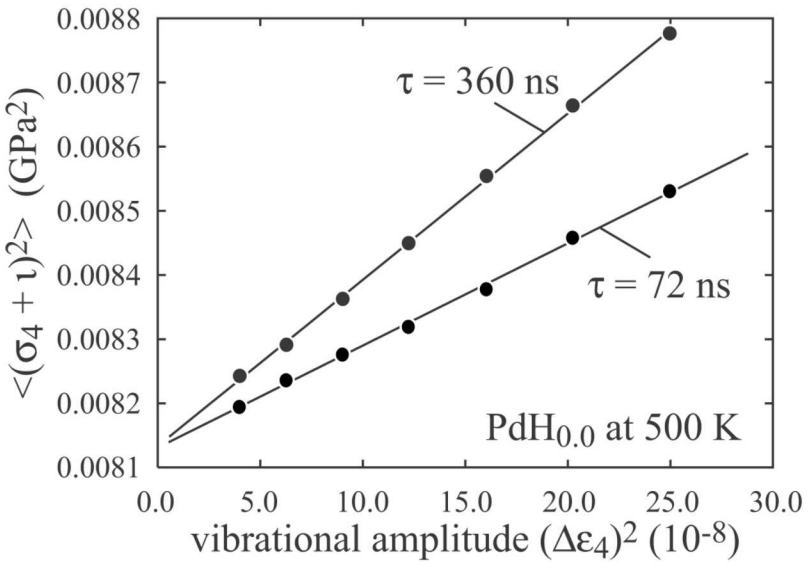

(b) $PdH_{0.7}$ $\langle(\sigma_4+\iota)^2\rangle$ vs. $\Delta\varepsilon^2_4$

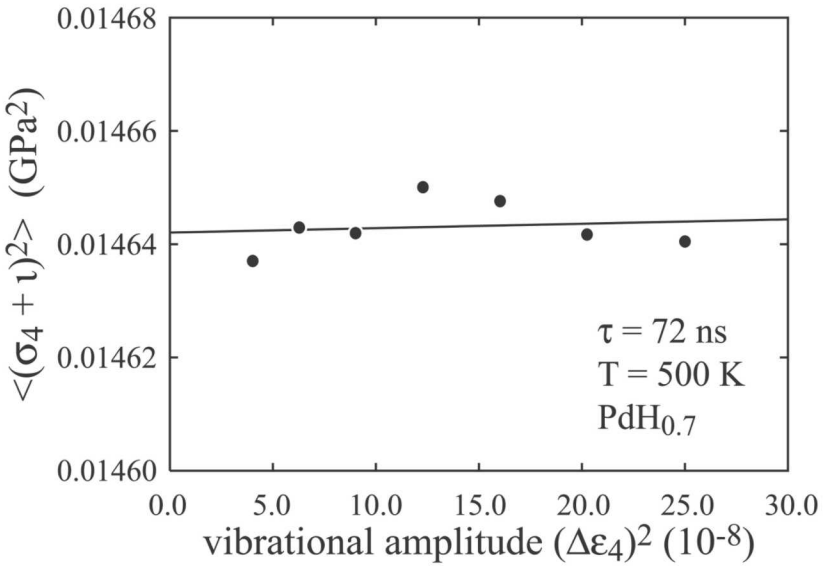

(c) Pd C_{44} vs. τ

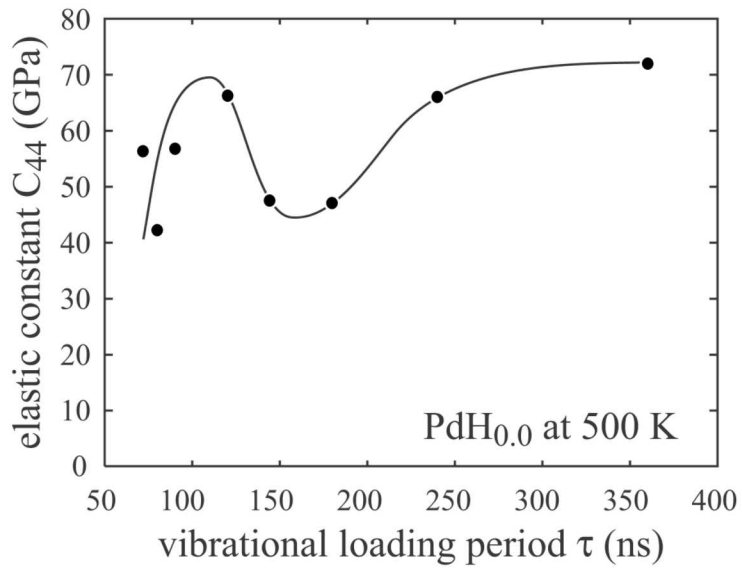

Linear relation is satisfied by Pd, but not by $PdH_{0.7}$

C_{44} depends on loading frequency

PdH_x: Mechanical Testing of Young's Modulus

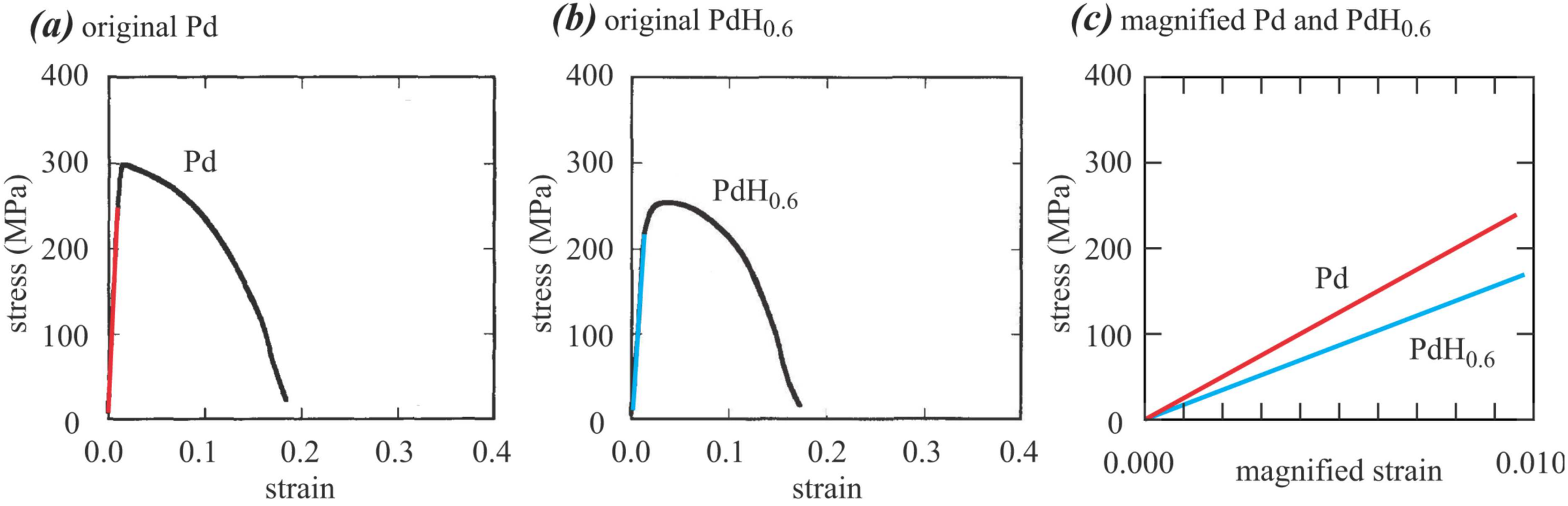

S. H. Goods and S. E. Guthrie, Scripta Metall. Mater. 26, 561 (1992)

- **Young's modulus of $PdH_{0.6}$ seems to be lower than that of Pd**
- **The resolution in experiments is too low to conclude**

PdH_x: Surface Segregation

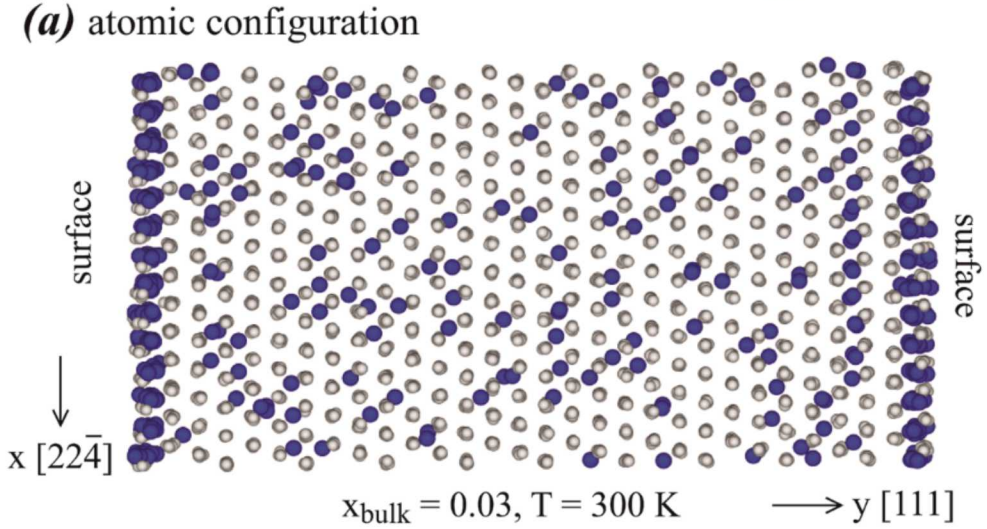

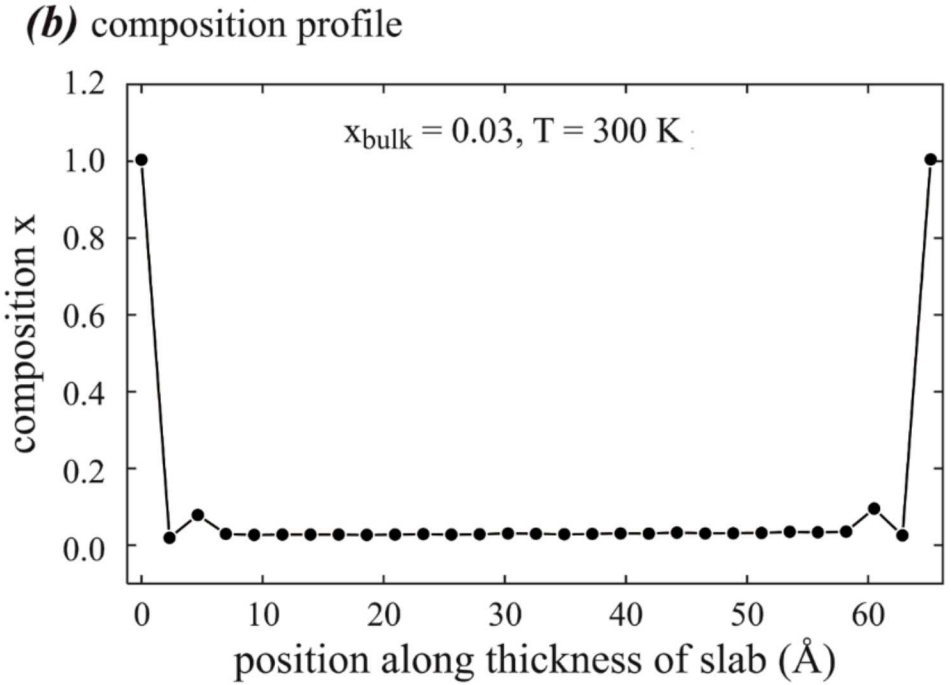

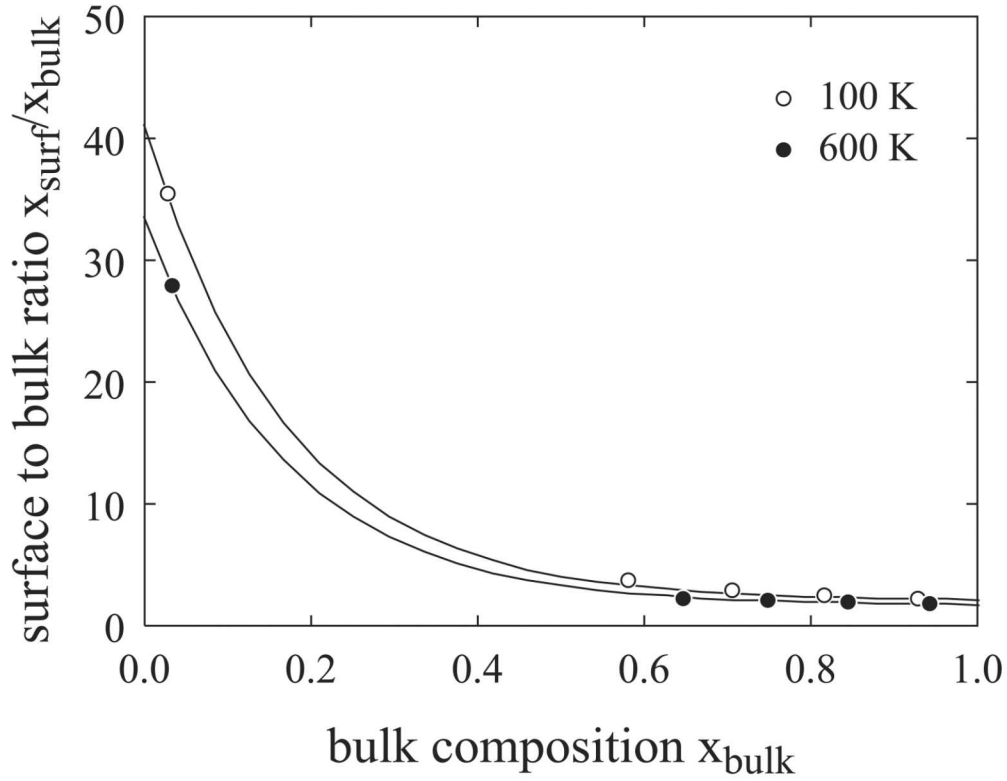

- **Time / ensemble average is key to the convergence**
- **H at {111} surface is ~30 times segregated**

Second Class: Transformational Hydrides

Case Study: MgH_x

MgH_x: Review of Potentials

- Literature Mg-H **EAM** potential by Ruda et al, ANALES DE LA ASOCIACION QUIMICA ARGENTINA, 84, 393 (1996)

Rutile Crystal for MgH_2

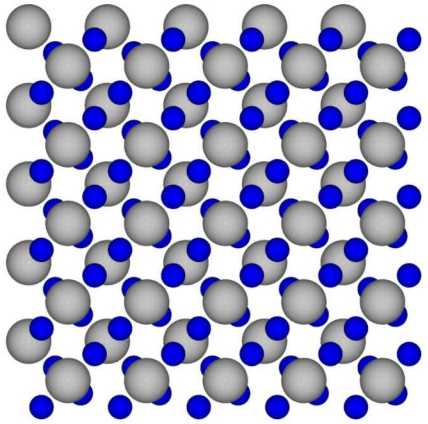

Molecular Statics At 0 K

⇒

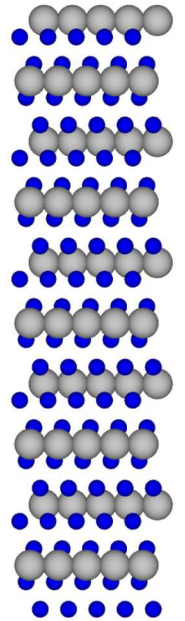

$(110)MgH_2$ // (0001) Mg, $[110]\ MgH_2$ // [2-1-10] Mg
Phil. Mag. Lett., 90, 1, 2010

- Literature Mg-H **ReaxFF** potential developed by S. Cheung, W. Q. Deng, A. C. T. van Duin, W. A. Goddard, J. Phys. Chem., 109, 851 (2005)

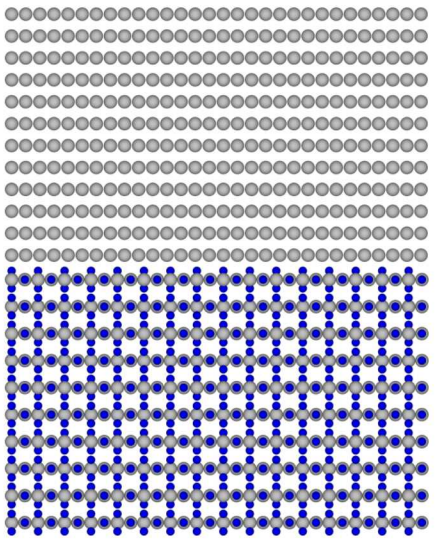

Molecular Dynamics T = 300 K t = 0.01 ns

⇒

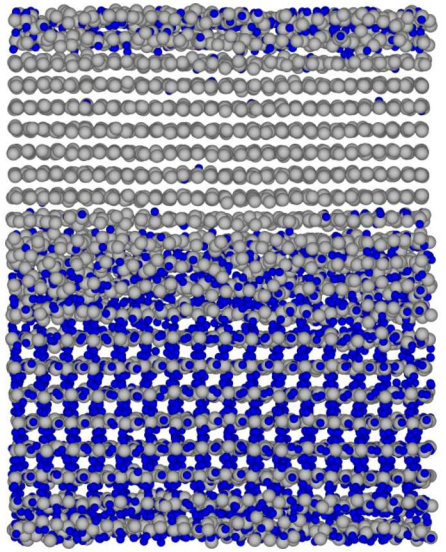

MgH_x: Analytical Bond Order Potential

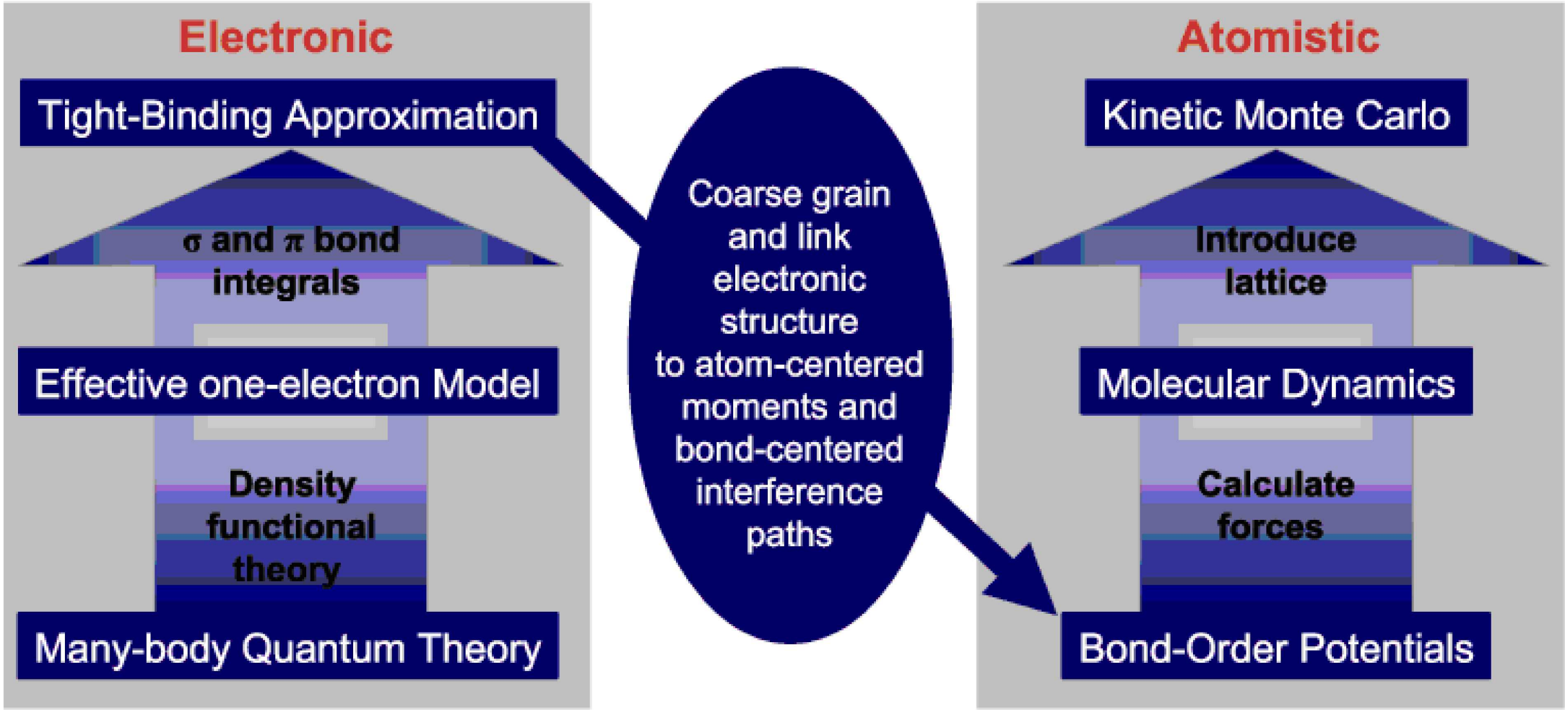

D. G. Pettifor et al, Mater. Sci. Eng. A, 365, 2 (2004)

MgH_x: H Component

Hydrogen crystal to H_2 gas

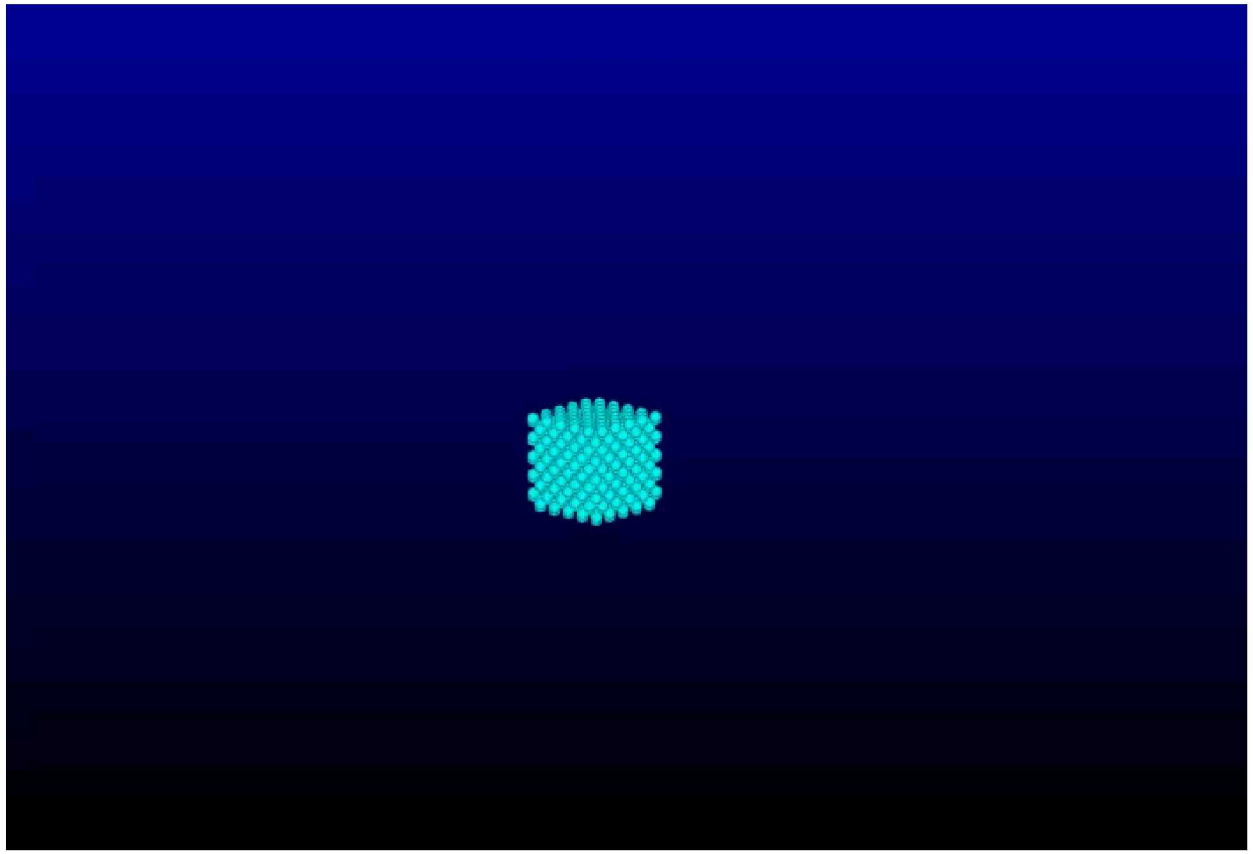

$H_2+H \rightarrow H+H_2$ energy profiles

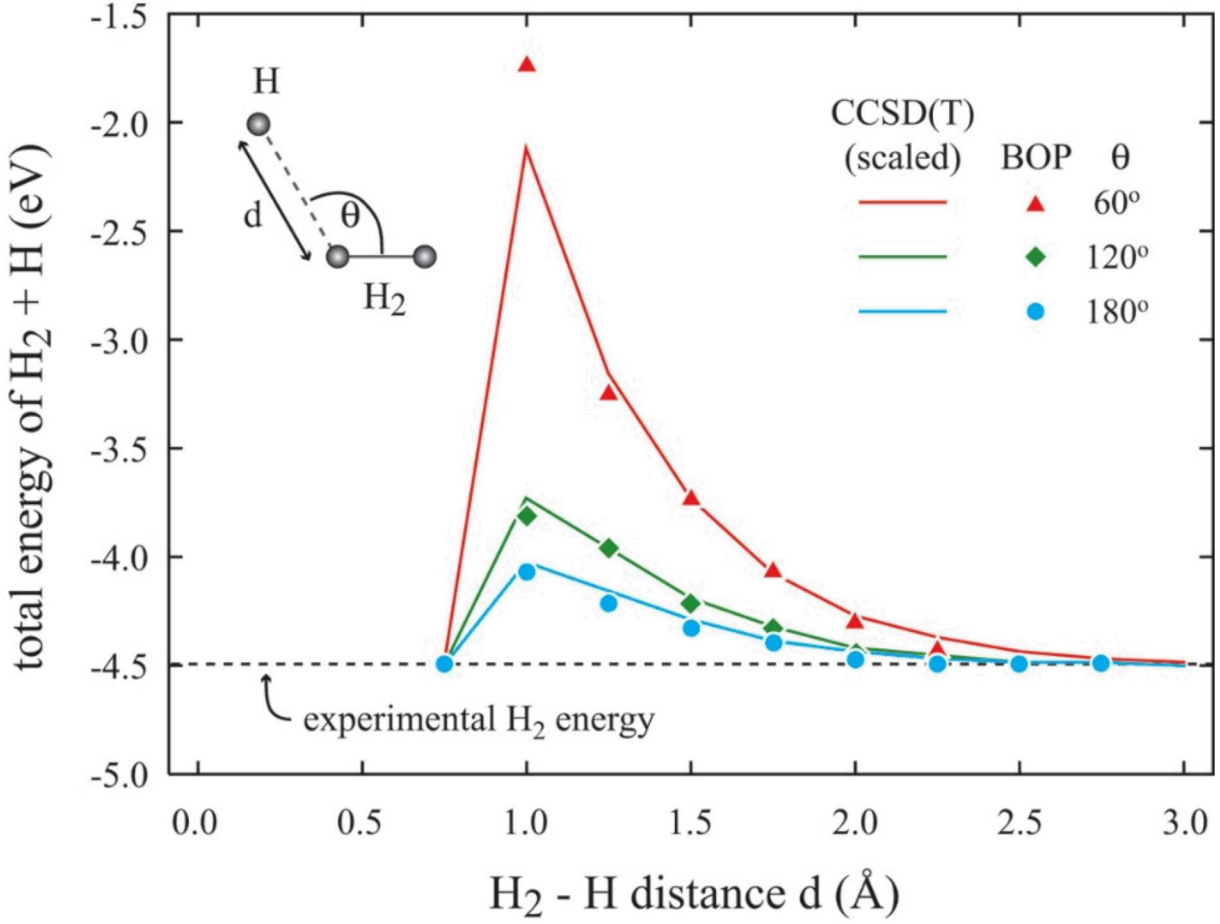

X. W. Zhou, D. K. Ward, M. Foster, J. A. Zimmerman, J. Mater. Sci., 50, 2859 (2015)

MgH_x: Transferability

Mg-hcp and MgH_2-rutile growth simulations

Energy / volume trends of phases

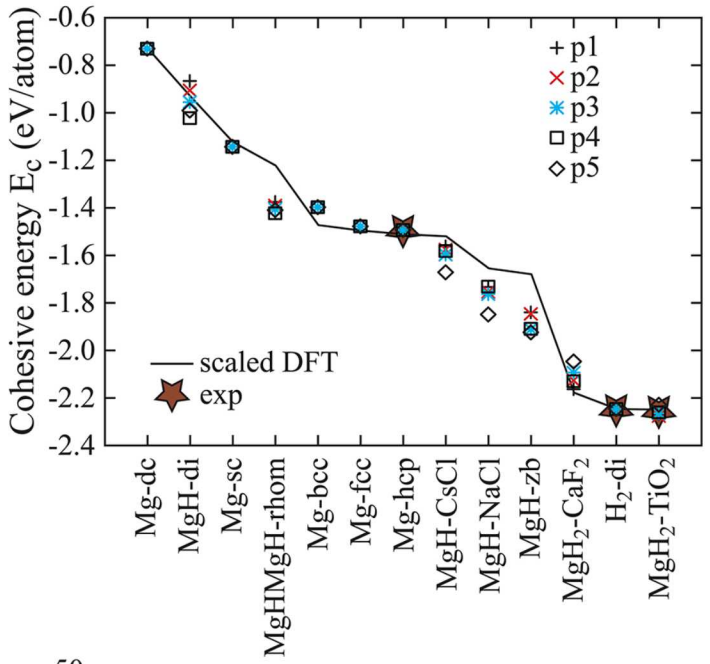

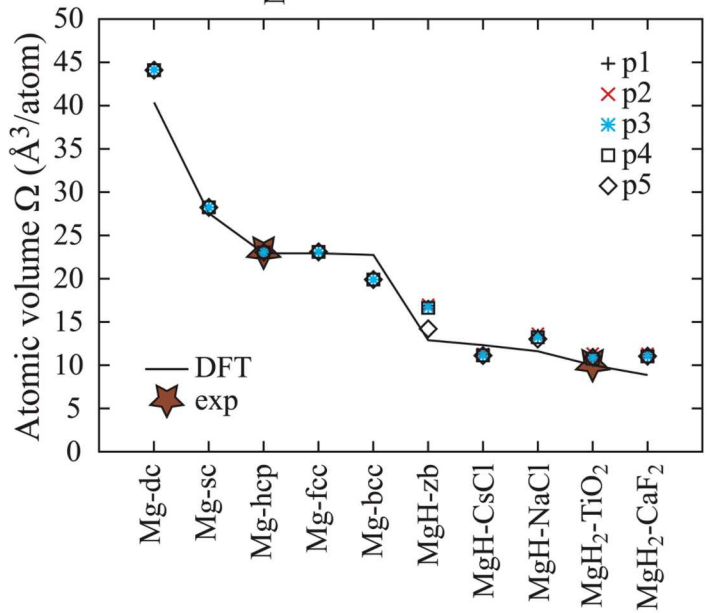

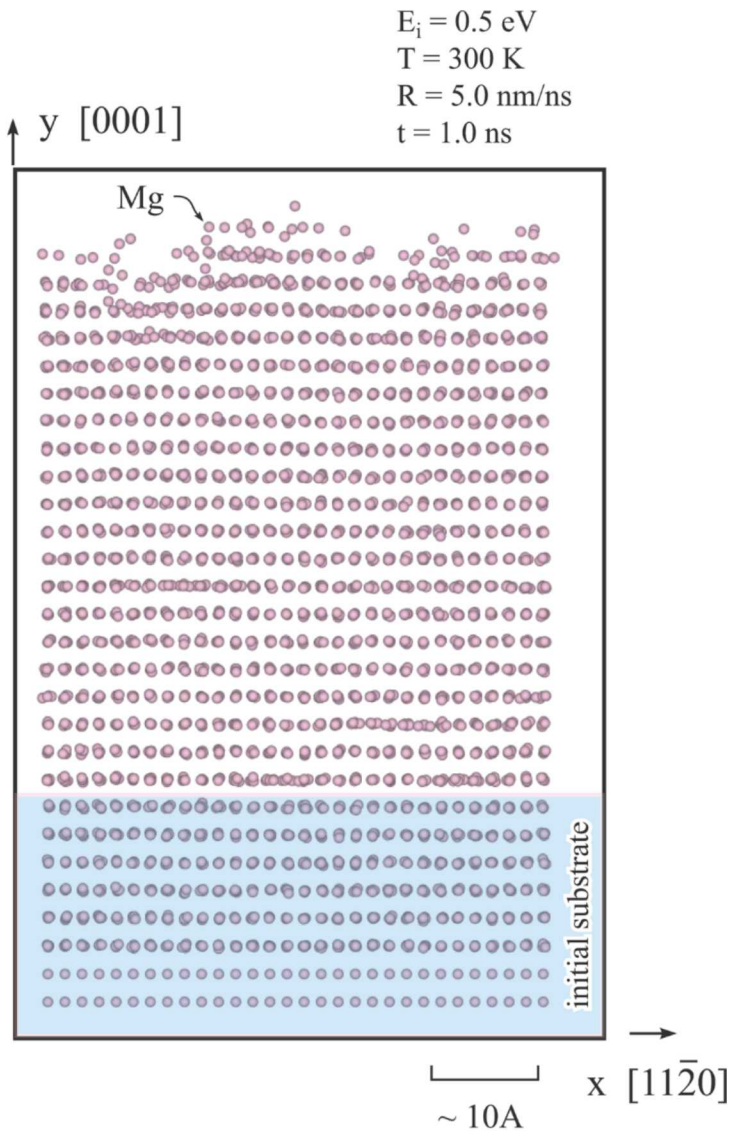

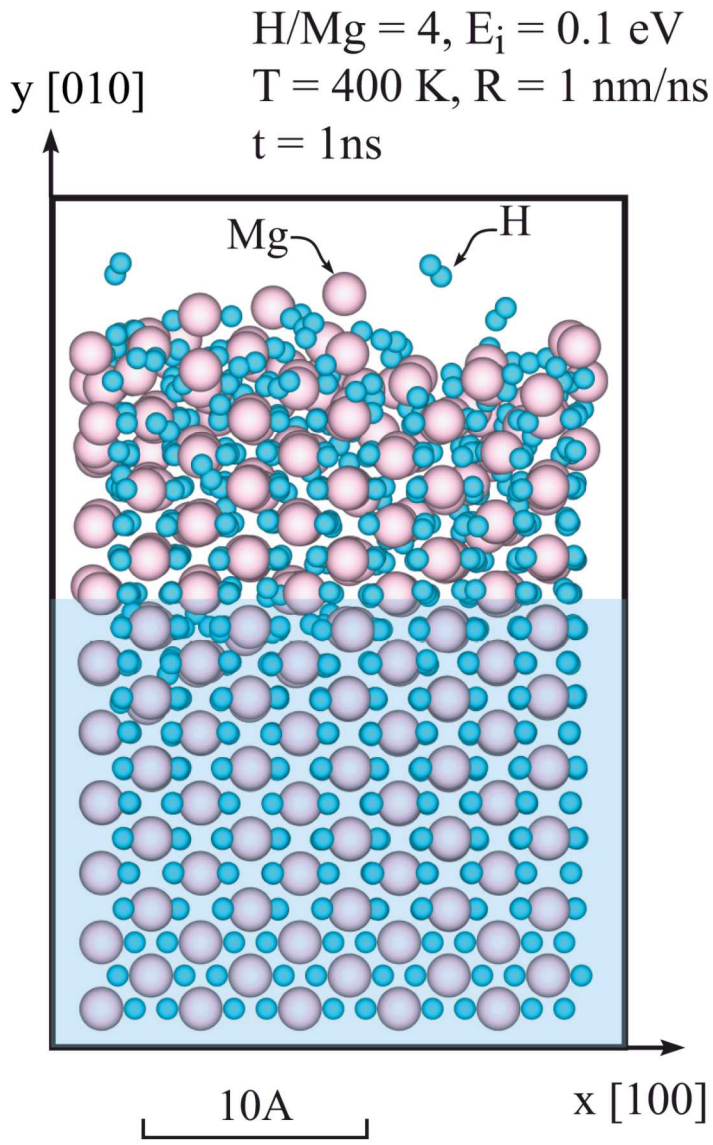

Third Class: Complex Hydrides

Case Study: MgB_xH_y

MgB_xH_y: Motivation

- LLNL is developing a phase field model for (de)hydrogenation kinetics of MgB_xH_y
- The phase field model requires thermodynamic and kinetic properties as inputs
- Many molecules may occur, and many exhibit amorphous structures ⇒ challenging for DFT studies
- We will use MD to fill the gaps

Example Molecules

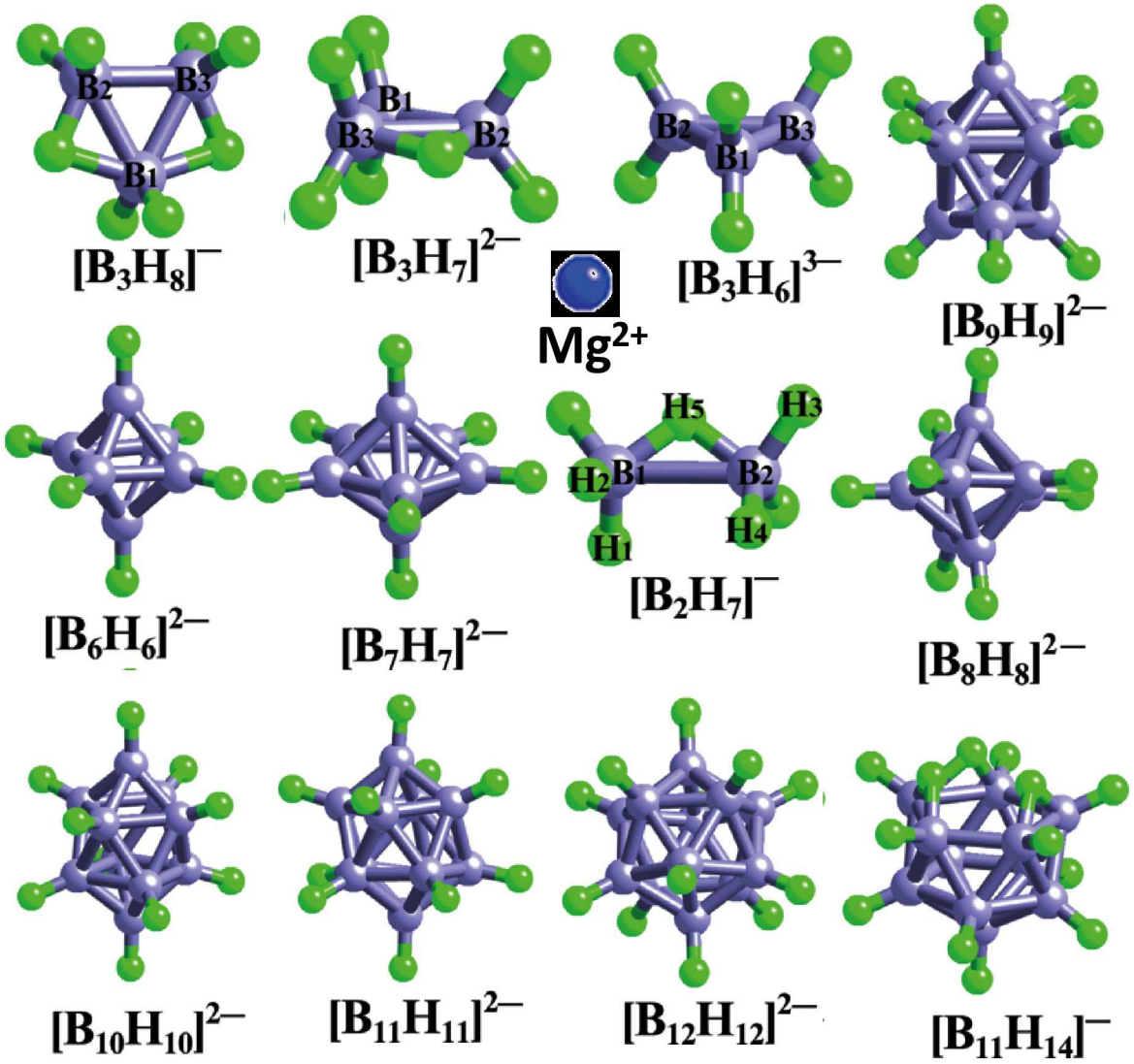

MgB_xH_y: Two Goals

$Mg(BH_4)_2 \Leftrightarrow MgB_2 + 4H_2 \ldots$

$MgB_{12}H_{12}$

$Mg(B_3H_8)_2$

$MgB_{10}H_{10}$

MgB_xH_y

…

- Many molecules were observed in NMR, XES, XAS, but not XRD ⇒ amorphous
- DFT is not sufficient for amorphous complex hydrides

Goal 1: Use MD to evaluate stabilities of different intermediates

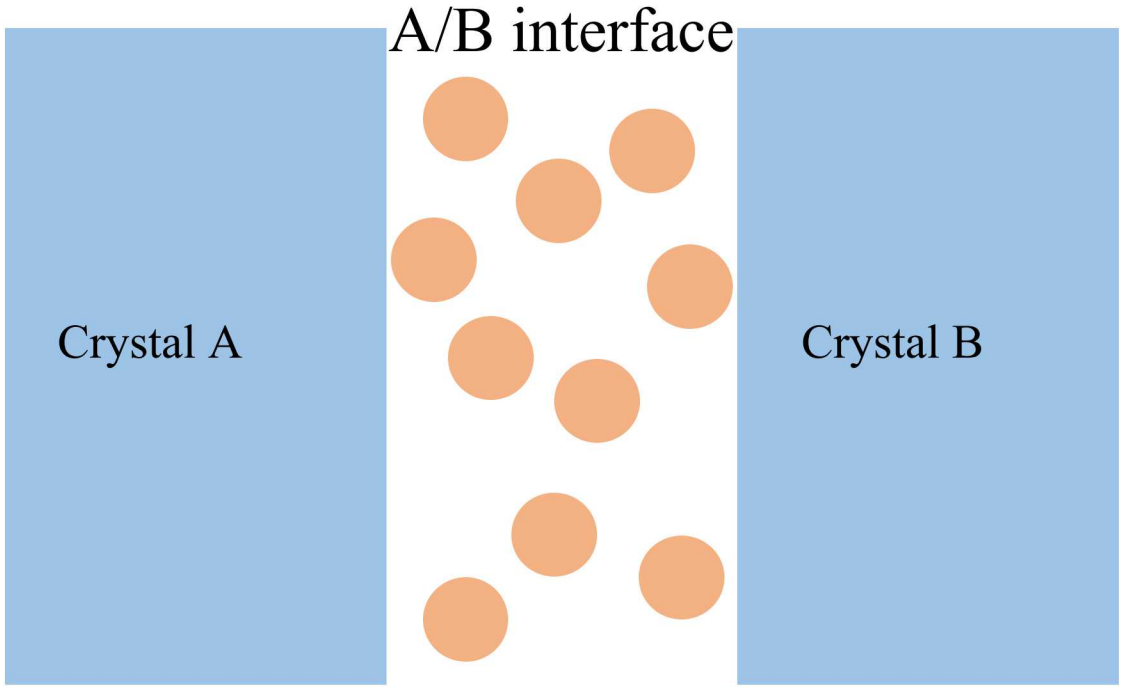

- Interfaces between crystalline solids are often exhibit amorphous "soup" containing different molecular species

Goal 2: Use MD to calculate interfacial energies

MgB_xH_y: "Molecular" Dynamics Simulations

Molecular Systems

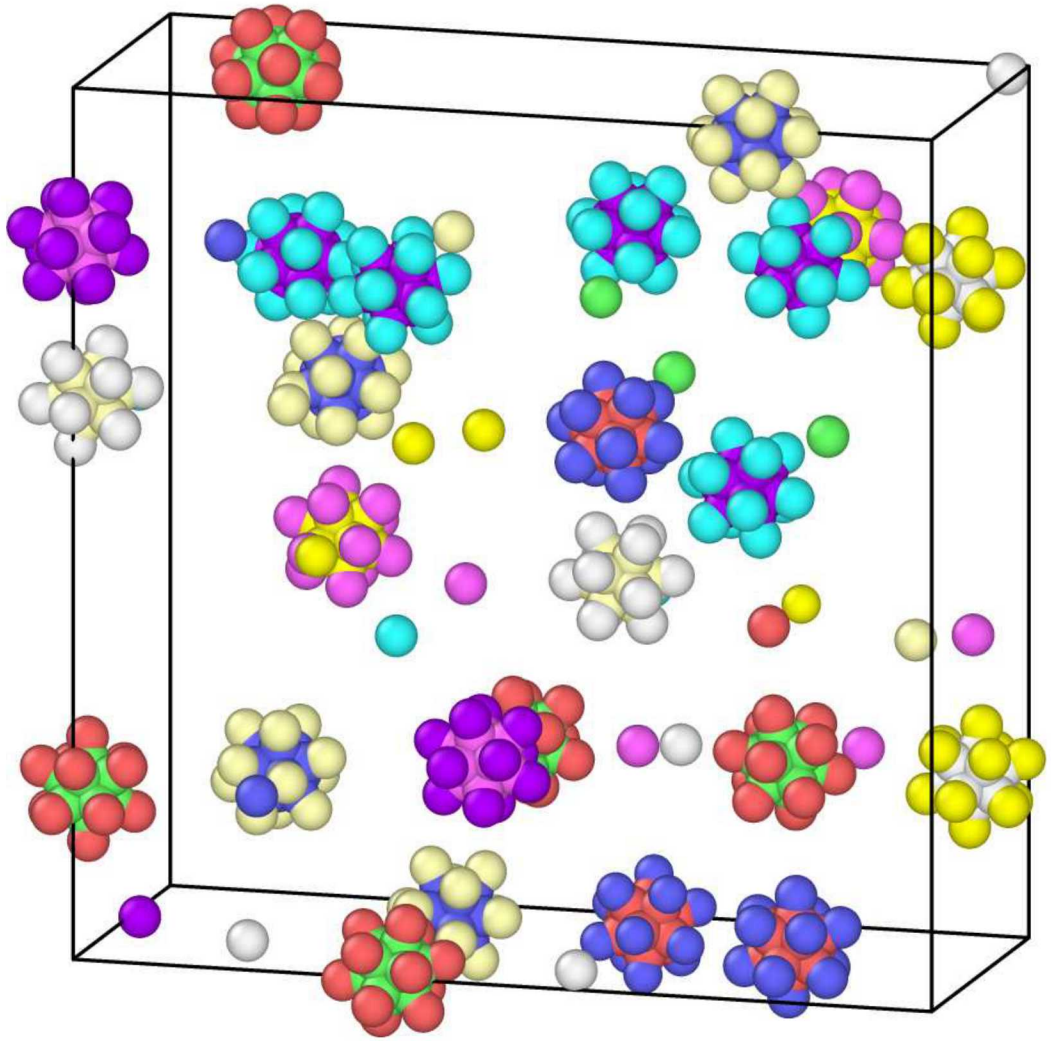

- Computational systems contain molecules rather than atoms
- Molecular forces equal sum of atomic forces between molecules
- In molecular dynamics simulations, species are distinguished by combination of molecules and atoms, not just atoms

Molecular and Atomic Forces

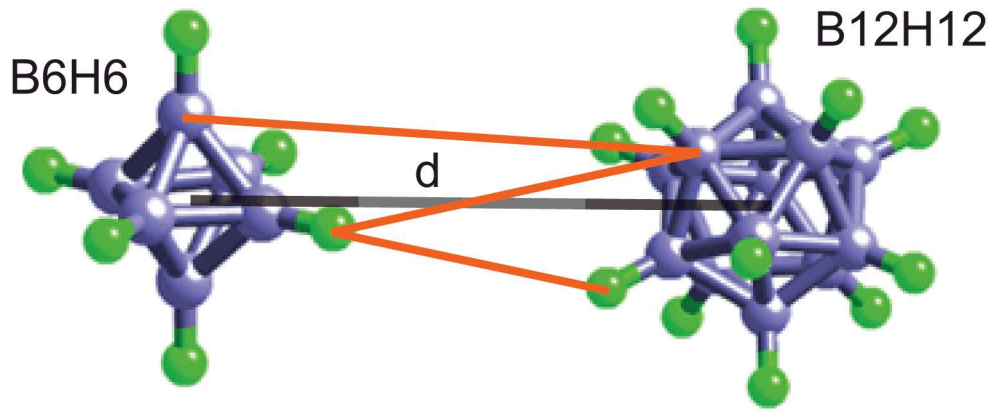

MgB_xH_y: Methods

- Energy comes from interactions between atoms from different (similar and dissimilar) molecules
- Perform DFT calculations of energies of all pairs of molecules at various distances and angles
- Fit pair potentials to DFT energies
- Implement the approach in LAMMPS

Interactions between different pairs of species are distinguished by rotation

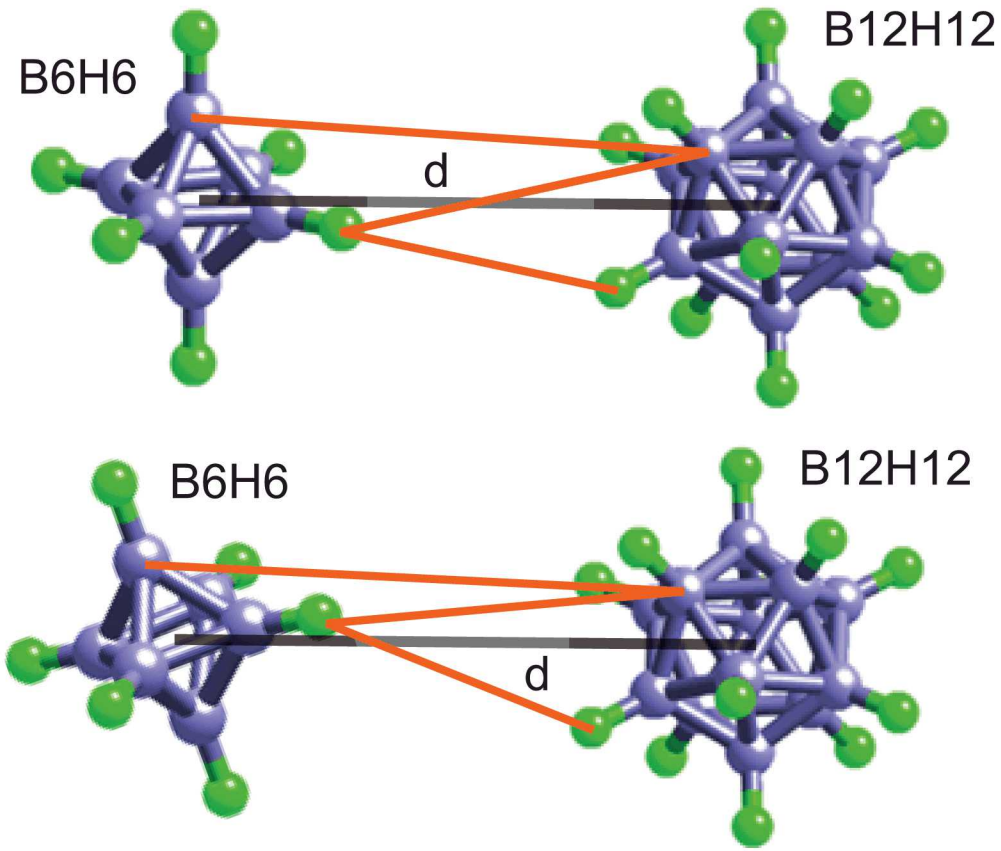

MgB_xH_y: Status

- Completed the Mg, H_2, BH_4, MgH_2, and $B_{12}H_{12}$ model
  - 36 interactions (intra-molecule interactions not included): Mg-Mg(Mg-Mg), Mg-H_2(Mg-H), Mg-BH_4(Mg-B,Mg-H), Mg-MgH_2(Mg-Mg,Mg-H), Mg-$B_{12}H_{12}$(Mg-B,Mg-H), H_2-H_2(H-H), H_2-BH_4(H-B,H-H), H_2-MgH_2(H-Mg,H-H), H_2-$B_{12}H_{12}$ (H-B,H-H), BH_4-BH_4(B-B,B-H,H-H), BH_4-MgH_2(B-Mg,B-H,H-Mg,H-H), BH_4-$B_{12}H_{12}$(B-B,B-H,H-B,H-H), MgH_2-MgH_2(Mg-Mg,Mg-H,H-H), MgH_2-$B_{12}H_{12}$(Mg-B,Mg-H,H-B,H-H),$B_{12}H_{12}$-$B_{12}H_{12}$(B-B,B-H,H-H)
- Adding B_3H_8 and $B_{10}H_{10}$ results in 42 additional interactions
- Adding $B_{11}H_{14}$ results in 27 additional interactions
- Ultimately we plan to perform MD studies on mixture of Mg, H_2, BH_4, MgH_2, $B_{12}H_{12}$, B_3H_8, $B_{10}H_{10}$, and $B_{11}H_{14}$

MgB_xH_y: Mg, H_2, BH_4, MgH_2, and $B_{12}H_{12}$ Modeling

- ✓ Completed DFT training sets on **H_2, Mg, MgH_2, BH_4, $B_{12}H_{12}$** (> 700 cases)
- ✓ Fitted all 36 interactions of these five molecules

Rotation Dependent Molecular Interaction

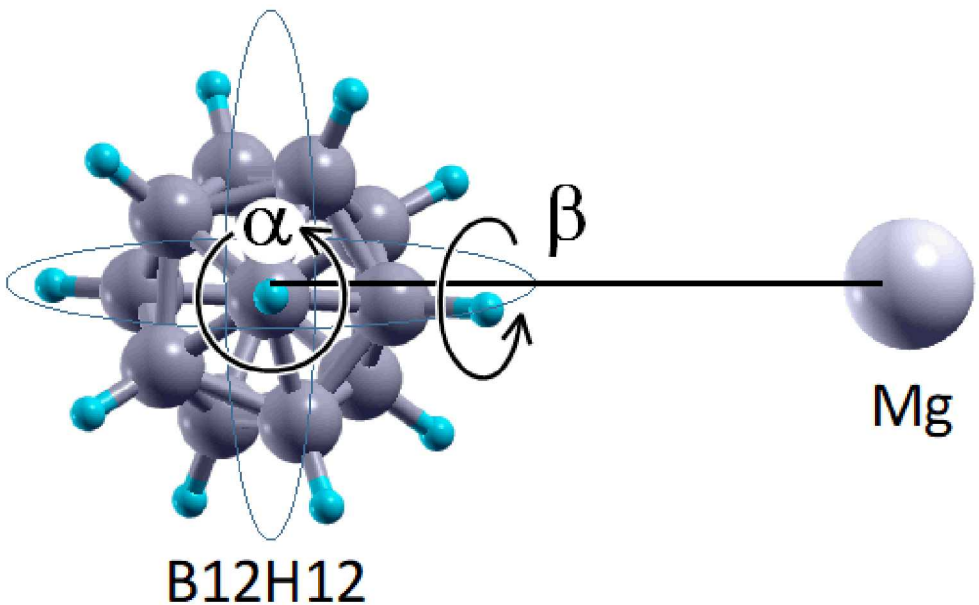

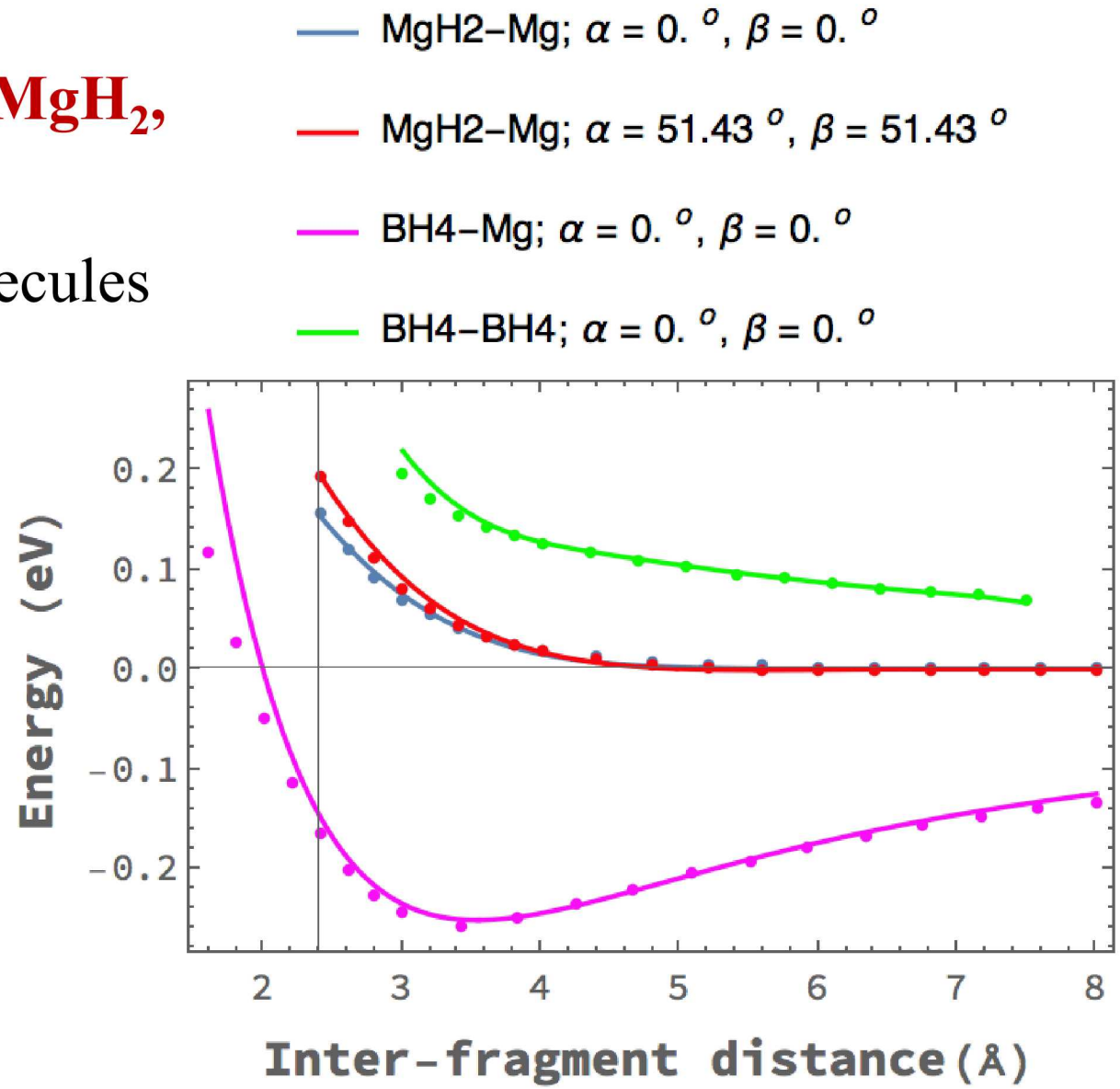

MgB_xH_y: "Molecular" Dynamics Simulation

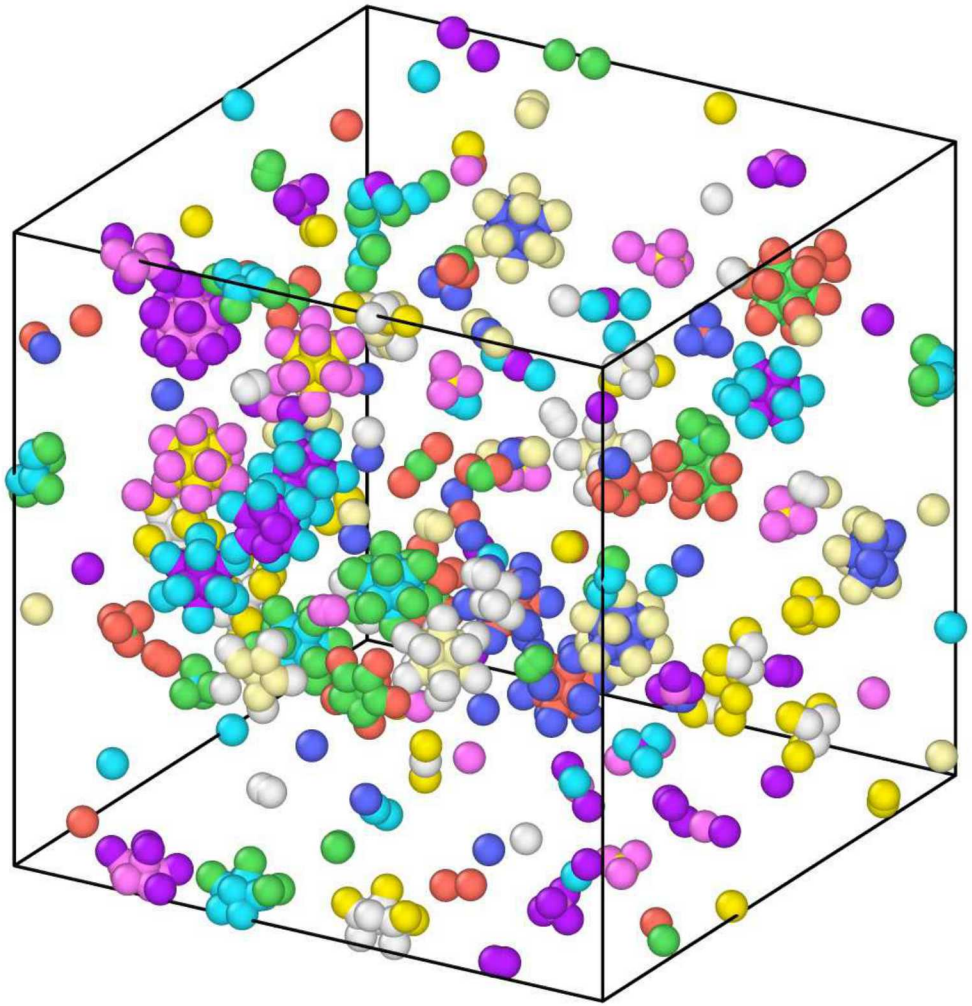

Highlights

- Robust MD tools have been developed for various classes of materials
- Lattice / elastic constants, Gibbs energy, surface / bulk diffusivities, surface / interface energies, surface segregation, are calculated in the entire temperature / composition space for PdH_x
- H diffusivity in PdH_x can be described by a two-barrier model
- Static shear elastic constants might be lower than ultrasonic elastic constants for H-rich PdH_x phase.
- Our Mg-H potential enables MD to examine MgH_2 formation mechanisms and extract related properties
- We have developed a "molecular" dynamics tool to study complex hydrides such as MgB_xH_y

Bulk Lattice Constant and Gibbs Free Energy

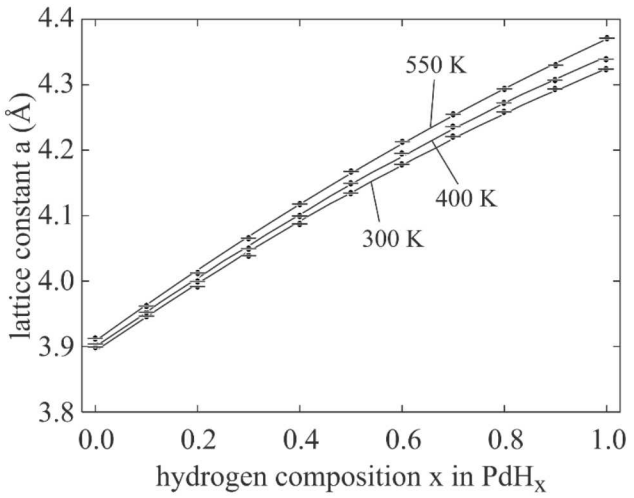

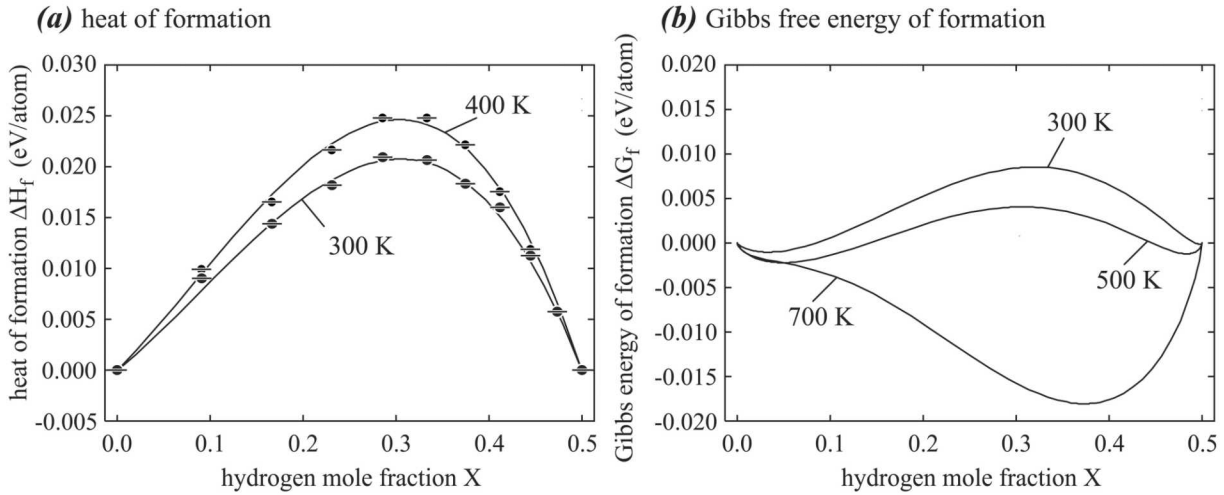

$$\begin{cases} a(x,T) = a_{300K} + a_{300K}\cdot\alpha\cdot(T-300) \\ a_{300K} = 3.8927 + 0.5360\cdot x - 0.1047\cdot x^2 \\ \alpha = 0.00001574 + 0.00002680\cdot x \end{cases}$$

- Experimentally, a_{300K} = 3.89 Å, α = 0.000012 K^{-1} (Griessen, R.; Strohfeldt, N.; Giessen, H. Nature Mater. **2016**, 15, 311-317), match well predictions
- However, experimental lattice constant of 4.09 Å for PdH at 77 K (Schirber, J. E.; Morosin, B. Phys. Rev. B **1975**, 12, 117-118), does not match predictions.

t_{MD} = 4.4 ns

$$\begin{aligned} \Delta H_f(X,T) = & \left(-0.6630 - 0.0837615\cdot T - 0.0679350556\cdot T^2\right)\cdot X\cdot(0.5-X) \\ & + \left(0.2405 + 0.1781152\cdot T + 0.1358574109\cdot T^2\right)\cdot X^2\cdot(0.5-X) \\ & + \left(1.7895 + 0.1660995\cdot T + 0.1358731023T^2\right)\cdot X\cdot(0.5-X)^2 \end{aligned}$$

$$\Delta S_f = -\frac{1}{1+x}k_B\left[x\ln(x) + (1-x)\ln(1-x)\right] = -k_B\left[X\ln\left(\frac{X}{1-X}\right) + (1-2X)\ln\left(\frac{1-2X}{1-X}\right)\right]$$

$$\Delta G_f(X,T) = \Delta H_f(X,T) - T\cdot\Delta S_f(X,T)$$

Over-predicted the β composition (Manchester, F. D.; San Martin, A.; Pitre, J. M. J. Phase Equilib. **1994**, 15, 62-83).

Surface/Interface Energies

Interface Energy Model

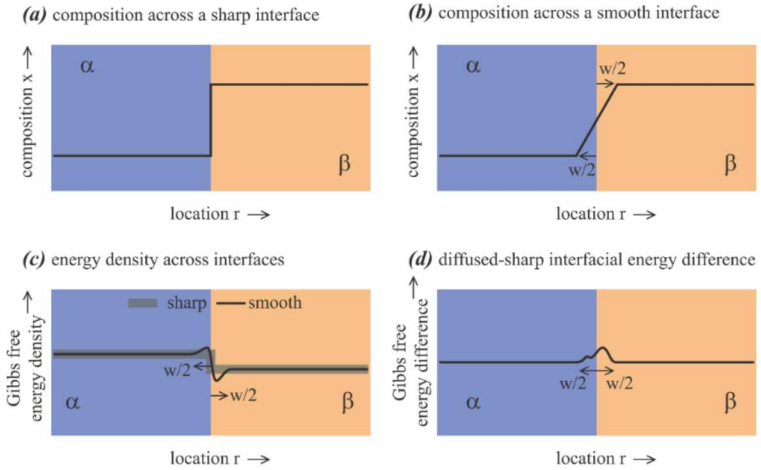

$$\gamma_i = \int_{-w/2}^{w/2} \frac{\Delta G_f(x,T) + E_e(x,T,f_\beta,x_\alpha,x_\beta)}{\Omega(x,T)} dr - \left[\frac{\Delta G_f(x_\alpha,T) + E_e(x_\alpha,T,f_\beta,x_\alpha,x_\beta)}{\Omega(x_\alpha,T)} + \frac{\Delta G_f(x_\beta,T) + E_e(x_\beta,T,f_\beta,x_\alpha,x_\beta)}{\Omega(x_\beta,T)} \right] \frac{w}{2}$$

f_β: volume fraction of β phase; x_α, x_β: compositions of α and β phases.

Interface Energy

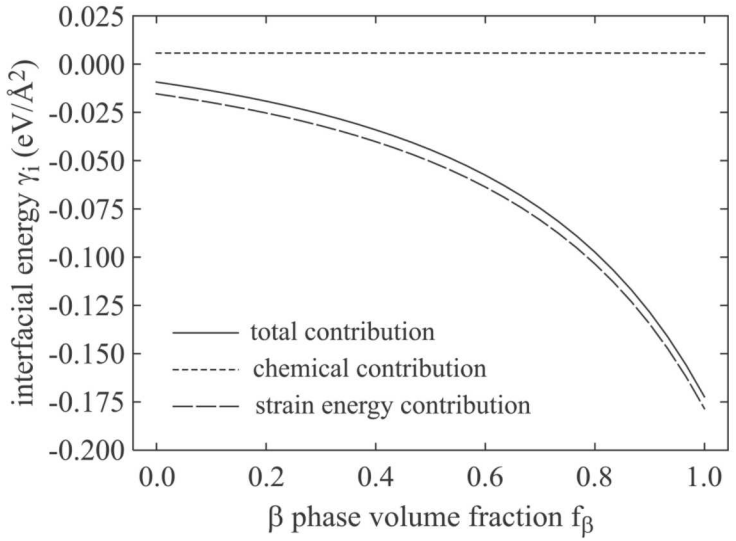

Surface Energy

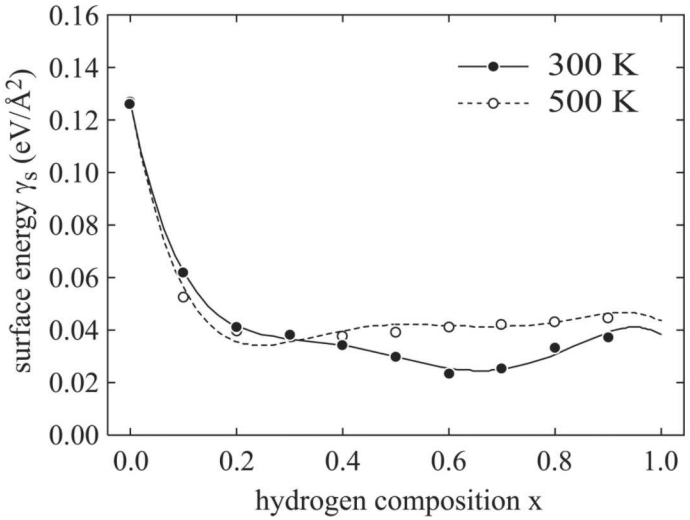

Interfacial energy as a function of β volume fraction at T = 300 K, x_α = 0.1, x_β = 0.9, and w = 15 Å.

Surface Diffusion

$t_{MD} = 3.3$ ns

MD Geometry

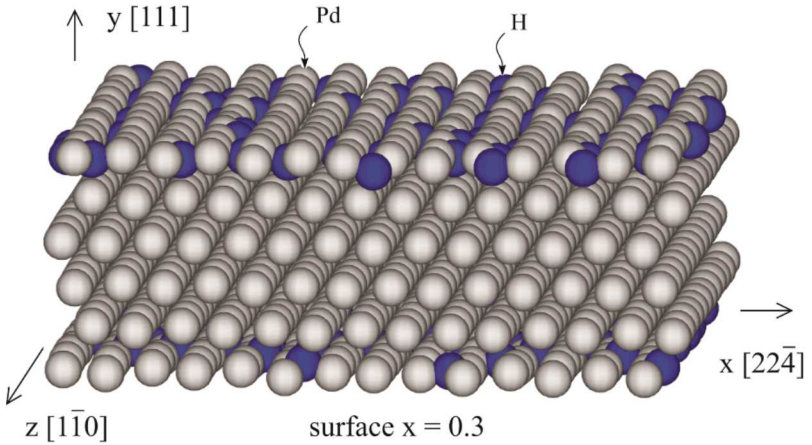

Diffusion Parameters

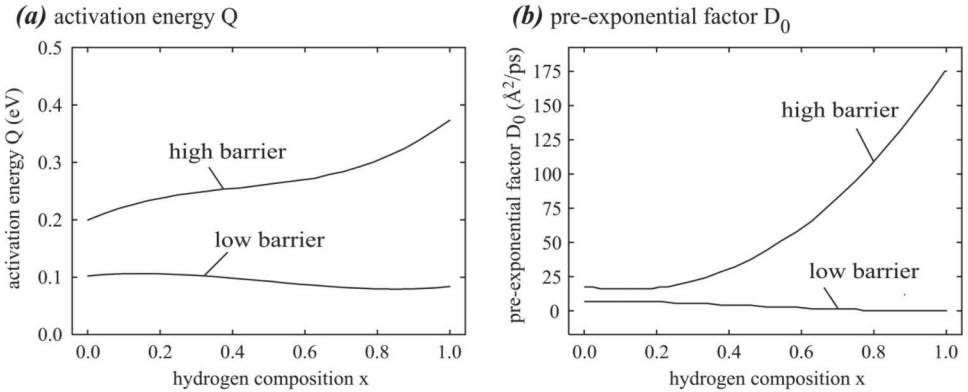

Arrhenius Plots

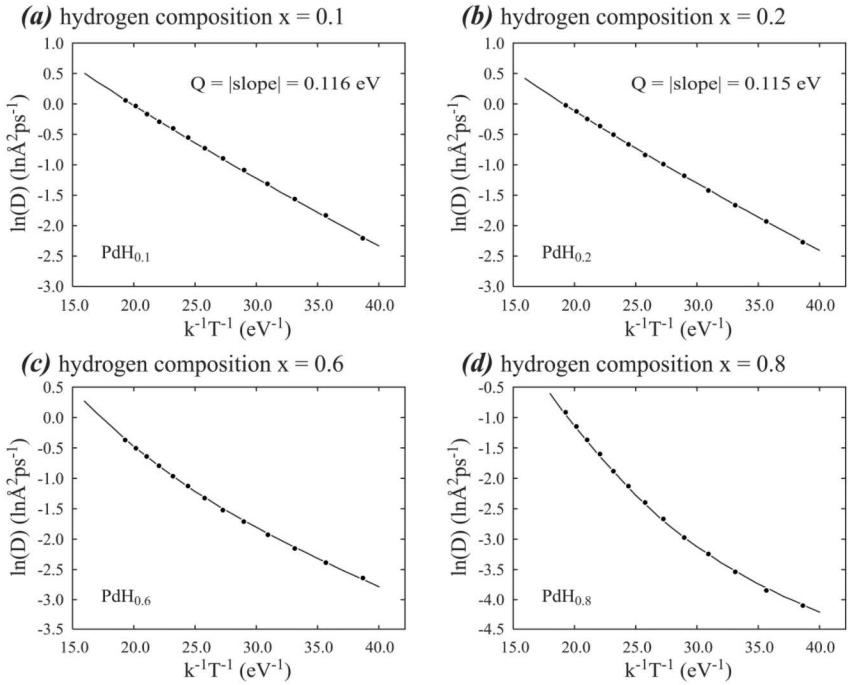

Nudged Elastic Band Calculations

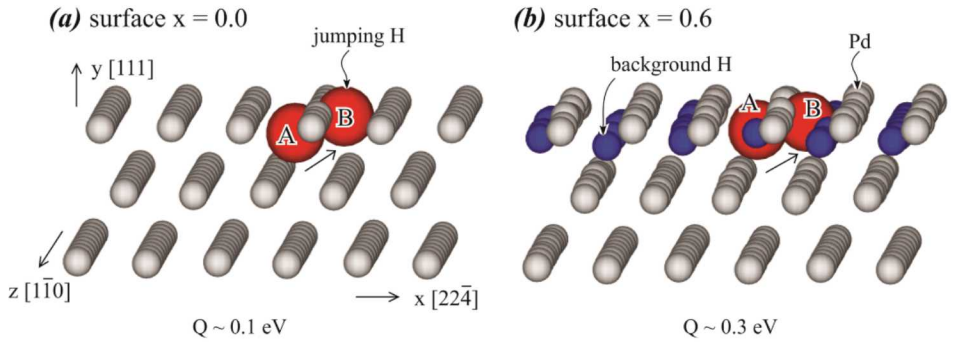

<u>MD reveals the same new diffusion mechanisms as bulk</u>

- Low H-composition has a single diffusion barrier because it is a dilute solution
- High H-composition has two diffusion barriers because the local H-composition varies
- This was confirmed by the nudged elastic band calculations